Climate change impacts on regional fire weather in heterogeneous landscapes of ~~Central~~ central Europe

Julia Miller[1,2,3], Andrea Böhnisch[4], Ralf Ludwig[4], and Manuela I. Brunner[1,2,3]

[1]Institute for Atmospheric and Climate Science, ETH Zurich, Zurich, Switzerland
[2]WSL Institute for Snow and Avalanche Research SLF, Davos Dorf, Switzerland
[3]Climate Change, Extremes and Natural Hazards in Alpine Regions Research Center CERC, Davos Dorf, Switzerland
[4]Department of Geography, Ludwig-Maximilians-Universität München, Munich, Germany

Correspondence: Julia Miller (julia.miller@slf.ch)

Abstract. Wildfires have reached an unprecedented scale in the Northern Hemisphere. The summers of ~~2021 and~~ 2022 and 2023 demonstrated the destructive power of wildfires especially in Northern America and Southern Europe. Global warming ~~indicates that fire seasons will~~ leads to changes in fire danger. Specifically, fire seasons are assumed to become more extreme and will extend to more temperate regions in northern latitudes in the future. However, the extent to which the seasonality and severity of fire danger in regions of central Europe will change in the future remains to be investigated. Multiple studies claim that natural variability ~~hides~~ and model uncertainty hide the trend of increasing fire danger in multi-model climate model simulations for future potentially fire-prone areas. Such trend might be isolated with Single Model Initial-Condition Large Ensembles (SMILEs) which help scientists to distinguish ~~climate trends~~ the forced response from natural variability. So far, the SMILE framework has only been applied for fire danger estimation on a global scale. To date, only a few dynamically downscaled regional SMILEs exist, although they enhance the spatial representation of climatic patterns on a regional or local scale.

In this study, we use a regional SMILE of the Canadian ~~regional climate model~~ Regional Climate Model version 5 (CRCM5-LE) over ~~Central~~ a region in central Europe under the ~~RCP 8.5~~ RCP8.5 scenario from 1980 to 2099 ~~, to analyze fire danger trends~~ to analyze changes in fire danger in a currently not fire-prone area. We use the ~~meteorological~~ Canadian Fire Weather Index (FWI) as a fire danger indicator. The study area covers four heterogeneous landscapes, namely the Alps, the Alpine Foreland, the lowlands of the Southern German Escarpment and the Eastern Mountain Ranges of the Bavarian Forest. We demonstrate that the CRCM5-LE is a suitable dataset to disentangle climate trends from natural variability in a multivariate fire danger metric. ~~Results~~ Our results show the strongest increases in the median (50^{th}) and extreme (90^{th}) ~~percentile~~ quantiles of the FWI in the northern, low-elevation parts of the study area in the summer months of July and August~~, where~~ . There, high fire danger becomes the median condition ~~and extremes~~ by the end of the century and high fire danger levels occur earlier in the fire season. The southern, Alpine parts of the study region are affected less strongly ~~, but due to weaker variability in these regions,~~ by changes in fire danger than the northern parts. However, they reach their time of emergence (TOE) ~~is reached there~~ in the early 2040's because of very low current fire danger. In the northern parts, the climate change trend exceeds natural variability only in the late 2040's. We find that today's ~~threshold for a 100 year FWI event ,~~ 100-year FWI event will occur every 30 years by 2050 and every 10 years by ~~2099.~~ the end of the century. Our results highlight ~~Central Europe's~~ the potential for

severe ~~fire events from a meteorological perspective and~~ future fire events in central Europe, which is currently little fire-prone, and demonstrate the need for fire management ~~in the near future even in temperate regions .~~ even in regions with a temperate climate.

1 Introduction

The ~~wildfire~~ fire seasons of 2021~~and~~ , 2022 and 2023 affected the northern hemisphere at an unprecedented scale. Especially ~~South-Eastern~~ Southern Europe and British Columbia (Canada) experienced multiple extreme fire events in terms of intensity, severity and damage ~~(Giannaros et al., 2022; Gillett et al., 2022)~~(i.e. Giannaros et al., 2022; Gillett et al., 2022). In Greece, five wildfires at the beginning of August 2021 burned an area of 94 000 ha, which corresponds to three times ~~the~~ its average annual burned area over the period ~~2008 to 2019~~ 2008–2019 (Giannaros et al., 2022). 90 % of the village Lytton in British Columbia (Canada) ~~was~~ were destroyed by fires in the summer of 2021 ~~during a heatwave caused by a blocking synoptic weather condition (Hoffman et al., 2022). While the Mediterranean region and the Western US are historically fire prone areas, Central Europe showed exposure to wildfires only in the recent years, e.g. in Treuenbritzen 2022, Brandenburg, Germany (Spiegel, 2022), and Küps 2022, Bavaria, Germany (BR, 2022).~~

~~In many~~ (Hoffman et al., 2022). In both cases, these fire events occurred under fire-favouring conditions of hot, dry and windy weather during the summer months. Summer heatwaves and drought events decrease soil moisture and increase the flammability of the vegetation prior to the fire event ~~(Ruffault et al., 2020)~~(e.g. Ruffault et al., 2020). Blocking synoptic conditions trap hot air over distinct areas and lead to extreme temperatures, which contribute to very high fire danger ~~(Hoffman et al., 2022) .~~ (e.g. Hoffman et al., 2022). While the Mediterranean region and Western Canada have been historically fire prone and well studied on a larger regional scale (e.g. Abatzoglou et al., 2021; Barbero et al., 2020; Ruffault et al., 2020; Barbero et al., 2015) , fire occurrence in the temperate climate regions of Europe has received less attention and is rather studied on a national than on a regional level (e.g. Bakke et al., 2023; Arnell et al., 2021; Fargeon et al., 2020).

Due to climate change, fire weather and hence the likelihood of fire events is projected to increase in several regions of the world – including historically less fire-prone areas – in the future (IPCC, 2021). From a meteorological perspective, the risk of igniting a fire increases with higher temperatures and wind speed and with lower relative humidity. Alterations in these variables ~~will~~ are projected to more than double the ~~risk of~~ frequency of occurrence of extreme fire weather until the end of the 21st century (Touma et al., 2021) and increase the duration, severity and spatial extent of fires ~~(De Rigo et al., 2017; Ruffault et al., 2020; Fargeon et~~ (Bowman et al., 2020; Fargeon et al., 2020; Ruffault et al., 2020; De Rigo et al., 2017).

~~Fire~~ Climate projections of fire danger often rely on fire indices, such as the Canadian Fire Weather Index (FWI) (van Wagner and Pickett, 1985), the National Fire Danger Rating Sytem (NFDRS) of the U. S. Forest Service (Bradshaw et al., 1984), ~~and~~ or the Australian McArthur Rating Sytem ~~(Mark 5) (McArthur, 1966) represent the statistical~~ (Mark 5; McArthur, 1966) . These indices are statistical models that were built on the correlation between fire events and meteorological conditions. They have been proven to produce reliable ratings of fire danger in short and long term weather predictions on a global scale ~~. However, these indices only describe the probability of a fire occurrence and do not guarantee an actual fire ignition~~

~~(Di Giuseppe et al., 2016). For~~ (Di Giuseppe et al., 2016). The FWI is the most commonly used index for assessing long-term fire ~~risk~~ danger with climate projections, ~~the FWI is the most commonly used index,~~ because it solely relies on meteorological inputs and does not propagate ambiguity from land use change (Touma et al., 2021). While this index describes the probability of a fire occurrence, it does not imply an actual fire ignition (e.g. Di Giuseppe et al., 2016).

~~Trends in fire risk show robust increases~~ Robust increases in future fire danger were simulated for Southern Europe and the Mediterranean region (IPCC, 2021)~~, but also in the Boreal zone, fire season length and fire frequency are projected to increase under climate change (Bakke et al., 2023).~~ . For example, Ruffault et al. (2020) have shown that under the ~~RCP 8.5~~ RCP8.5 emission scenario, the frequency of ~~heat induced~~ heat-induced wildfires will increase by 30% in the Mediterranean region ~~by the end of the century. Fargeon et al. (2020)~~ and Fargeon et al. (2020) have found that under ~~RCP 8.5~~RCP8.5, today's 10 year FWI maxima in France are reached every second year ~~in the future in France. In Central Europe, trends related to fire danger are uncertain and~~ by the end of the century. In contrast to the Mediterranean, temperate climate regions, such as central and western Europe, show uncertain trends in fire danger because these trends are not clearly distinguishable from ~~natural variability . Arnell et al. (2021) and Fargeon et al. (2020) have shown for England and France, respectively, that this~~ internal variability when multi-model climate ensembles are used (Arnell et al., 2021; Fargeon et al., 2020). This uncertainty originates from ~~an under-representation of natural variability in climate~~ the confusion of internal variability with structural uncertainty related to the different climate models in the ensemble (Arnell et al., 2021; Fargeon et al., 2020). Separating the forced signal in FWI changes from internal variability using multi-model ~~ensembles. In France, future fire danger exceedance of inter-annual variability decreases from South to North (Fargeon et al., 2020). Arnell et al. (2021) assessed the effects of climate change on fire danger indicators for the UK and found that the magnitude of fire danger change is hidden by the large natural variability of the input variables of the fire danger index and the differences between the different climate multi-model ensembles. Both studies highlight the importance of quantifying the natural variability of changes in future fire weather and its relevance for decision making with respect to fire risk mitigation and planning. However, it is challenging to properly quantify natural variability with multi-model~~ ensembles ~~for~~ only is challenging, in particular in temperate climate regions ~~(Arnell et al., 2021; Fargeon et al., 2020)~~with a low signal to noise ratio (Arnell et al., 2021; Fargeon et al., 2020; De Rigo et al., 2017) .

This ~~limitation, i. e. the under-representation of natural variability in fire danger estimates in regions with currently temperate climate, can be overcome~~ challenge can be addressed by evaluating climate model simulations derived from a single model initial-condition large ensemble (SMILE) which enables a clear isolation of the forced climate change signal from internal variability (Deser et al., 2012). SMILEs represent an ensemble of simulations derived using one single climate model started at different initial conditions. ~~This allows SMILEs to account for the internal variability~~ The ensemble spread between the different SMILE members provides a robust estimate of the internal variability, from which the forced response of the climate ~~system (Maher et al., 2021; Kay et al., 2015; Deser et al., 2012). Touma et al. (2021) successfully attributed changes in fire danger to anthropogenic greenhouse gas increases by analysing results from the global Community Earth System Model Large Ensemble.~~ change scenario can be estimated by averaging over the SMILE members for a specific variable, e. g. temperature (Deser et al., 2020). While single SMILEs allow for the quantification of internal variability, they do not enable a quantification of model uncertainty (Deser et al., 2020). Most of the available SMILEs rely on global circulation or ~~global~~ earth system models with a coarse spatial resolution and are unsuitable to assess changes in fire weather over regions with complex ~~terrain such as Central~~ terrain such as central Europe including the Alps.

In this study, we therefore use the CRCM5-LE, a ~~regionally downscaled,~~ dynamically downscaled, regional, high-resolution SMILE (0.11° grid cell size) nested into the CanESM2-LE (Fyfe et al., 2017), to disentangle climate change induced fire danger trends from ~~natural~~ internal variability over heterogeneous landscapes in ~~Central Europe. First, we~~ central Europe. Benefits of using a regional instead of a global SMILE are, among others, spatial representations of climatic patterns in high geographical detail, such as pressure patterns leading to extreme precipitation (Mittermeier et al., 2019) or heat waves (Böhnisch et al., 2023), and the seasonality of these extremes (Felsche et al., 2023; Böhnisch et al., 2021; Wood and Ludwig, 2020) .

We first assess the suitability of the ~~dataset~~CRCM5-LE, consisting of 50 climate model members, to reproduce typical FWI characteristics ~~which are similar to the~~ over central Europe. To do so, we compare FWIs computed from CRCM5-LE to an ERA-5-based FWI benchmark ~~provided by Vitolo et al. (2020)~~ (Vitolo et al., 2019) for the present time period (~~1980–2009). The~~ 1980–2009). Second, we use the unique setup of the CRCM5-LE ~~allows us to further~~ to evaluate how fire danger ~~increases~~ changes in the future under the ~~RCP 8.5~~ RCP8.5 greenhouse gas emissions scenario~~by taking internal variability into account. Second, we test the following hypotheses on future fire weather trends in the study area: (H1) The spatio-temporal development of the FWI~~ . Specifically, we address three research questions (RQ): (1) How does the FWI in central Europe change between 1980 and 2099 in ~~Central Europe increases significantly in~~ four hydro-climatologically diverse subregions~~; (H2) the~~ ?; (2) when does the FWI reach its time of emergence (TOE)~~is reached latest by 2099~~?; and (~~H3)~~ 3) how often does today's 100-year FWI ~~occurs at least every fifty years~~ occur by the end of the century~~.~~ ?

2 Data and ~~Methods~~methods

2.1 ~~CRCM5-LE~~CRCM5 large ensemble

To quantify changes and ~~natural~~ internal variability in fire danger ~~trends for Central~~ for central Europe, we use the Canadian Regional Climate Model version 5 Large Ensemble ~~(~~(CRCM5-LE; Leduc et al., 2019). The CRCM5-LE ~~) of Leduc et al. (2019). The dataset consists of 50 members at a spatial resolution of 12 km and was generated~~ was obtained by nesting the regional climate model CRCM5 (Šeparović et al., 2013; Martynov et al., 2013) into the CanESM2-LE (Fyfe et al., 2017) over two domains (i. e., Europe and Northeast America). Thereby, the CanESM2 was dynamically downscaled from an original resolution of 2.88° to 0.11° over these regions. The dynamical downscaling of a regional single-model initial condition large ensemble (SMILE) was carried out within the ClimEx project (https://www.climex-project.org/) to assess the hydrological impacts of climate change in Bavaria and Québec. ~~It~~ The dataset includes continuous simulations of climate variables from 1950 to 2099 under the RCP8.5 emission scenario ~~over two domains in Europe and Northeast North America (Leduc et al., 2019)~~(Leduc et al., 2019).

The ~~CRCM5-LE is derived from the~~ driving CanESM2-LE consists of 50 simulations (Fyfe et al., 2017), which ~~was created by applying small random perturbations at two different points in time (i. e. 1850 and 1950) to a 1000-year equilibrium~~

~~climate simulation under pre-industrial conditions (Leduc et al., 2019). In a first step, small random atmospheric perturbations were added to the equilibrium run to obtain five historical simulation families starting in 1850. In a second step, ten random perturbations were added to each family, resulting in a~~ were started by adding random perturbations to the initial atmospheric state of January 1st in 1950. These random perturbations were introduced by parameterizing a single aspect of the model's cloud properties using a different pre-set seed for each of the 50 ~~member ensemble~~simulations. This ensured that the climate change realizations were different from each other without changing the model dynamics, physics, or structure (Fyfe et al., 2017). After a 5-year spin-up phase, the modeled climate of the initialized 50 members ~~can be regarded as independent . This global SMILE was dynamically downscaled using the CRCM5 (Martynov et al., 2013; Šeparović et al., 2013) to obtain the regional SMILE~~ in the CRCM5-LE ~~(Leduc et al., 2019)~~were considered independent (Leduc et al., 2019), because the chaotic climate properties caused diverging climate trajectories soley based on the macro- and micro-initialization of the CanESM2-LE (Wood, 2023). Therefore, the differences among the 50 CRCM5-LE members can be interpreted as natural variability (Böhnisch et al., 2021; Wood, 2023; , and are referred to as internal variability throughout this paper (Hawkins and Sutton, 2009). For more details on the ensemble setup, the reader is referred to Leduc et al. (2019) (CRCM5-LE) and Fyfe et al. (2017) (CanESM2-LE).

~~Our analysis considers the period 1980 to 2099. At this time, all members share the same climatology and span a range of possible climate realizations, which give insights into the internal climate variability of the model (Leduc et al., 2019). In this study, we interpret internal variability as natural variability (Böhnisch et al., 2021; von Trentini et al., 2019; Kay et al., 2015).~~ A comparison between the CRCM5-LE and a multi-model ensemble (i. e. EURO-CORDEX) was conducted by von Trentini et al. (2019). Their results have shown ~~,~~ that the CRCM5-LE shows a smaller member spread for temperature and equal member spread for precipitation than EURO-CORDEX~~(von Trentini et al., 2019). The~~ . Further, the CRCM5-LE was bias corrected ~~over the study area for the FWI input variables at a three-hourly resolution using the~~ using the univariate quantile mapping approach of Mpelasoka and Chiew (2009) (Poschlod et al., 2020) ~~. Bias corrected data are~~ for all the FWI input variables. Bias-corrected data have been commonly used for projections of fire weather indicators ~~like the FWI (e. g. Yang et al. (2015), Kirchmeier-Young et al. (2017), Ruffault et al. (2020), Fargeon et al. (2020)), because frequencies of FWI extremes are significantly better represented than in non-bias-corrected climate data (Yang et al., 2015).~~ such as the FWI (e. g. Yang et al., 2015; Cannon, 2018; Kirchmeier-Young et al., 2017; Ruffault et al., 2017; Fargeon et al., 2020), as they have been shown to reflect fire danger more accurately than raw climate data when compared to observational data (Yang et al., 2015). For the bias correction, the meteorological Sub-Daily Climatological REFerence dataset (SDCLIREF), which combines hourly and disaggregated daily station data (Brunner et al., 2021), served as an observation reference. Correction factors were determined for each quantile bin of each month and sub-daily time step by pooling data across all members. The correction factors were applied separately to each member of the CRCM5-LE (Brunner et al., 2021).

2.2 Study ~~Area~~area

Our study ~~assesses~~ assessed changes in fire danger over a ~~hydro-climatologically~~ hydro-climatically diverse region in ~~Central~~ central Europe with temperate climate (Figure 1). The boundaries of the study area ~~are~~ were set by the river catchments of the Danube, Main and Elbe, which intersect with the German federal state of Bavaria. ~~The~~ As the study area exceeds the boundaries of political Bavaria in terms of these catchmentsand is therefore further , it is referred to as "Hydrological Bavaria" , short HydBav(HydBav). HydBav has an overall size of approximately 103 ,200 km^2. We divide divided HydBav into four subregions according to their geography and climatology: (1) The Alps in the South, (2) the Alpine Foreland north of the Alps bounded by the course of the Danube, (3) the Southgerman Escarpment north of the course of the Danube and (4) the Eastern Mountain Ranges of the Bavarian Forest in the East of the study area (s. figure see Figure 1). This subdivision into complex landscapes is was adopted from the ClimEx-Project and the study of Willkofer et al. (2020) and derived from the Bavarian State Office for the Environment (Landesamt für Umwelt, 2023). Since fire is closely related to the availability, or rather the absence of water , we assume (in terms of precipitation or soil moisture deficit), we assumed that the water availability, climatology and landscape of different river systems reflect the fire regime of an areacharacteristics of the four different complex landscapes resulted in subregion-specific fire regimes.

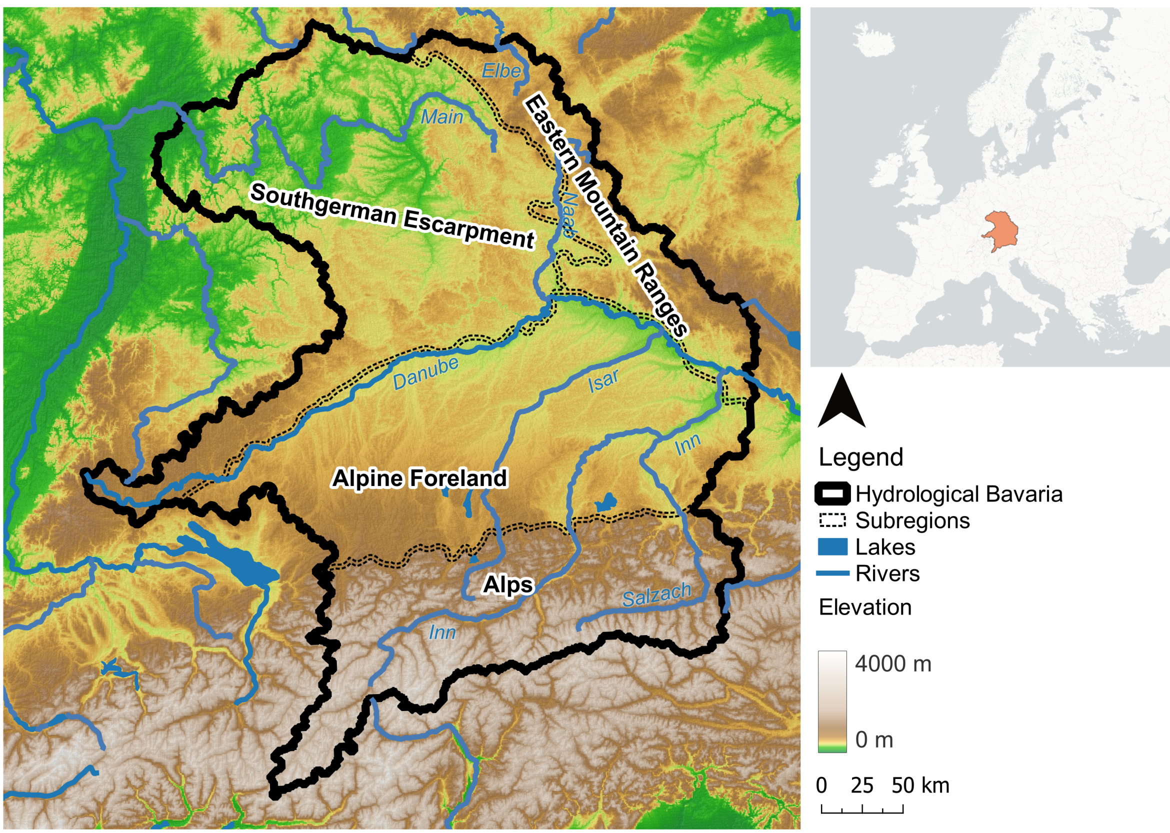

Figure 1. Subregions of Hydrological Bavaria by landscapes and land cover of Hydrological Bavaria (modified, CLMS (2021))

Figure 1 gives a brief overview of HydBav and its four subregions. According to the present climate period between 1980 and 2009 (present), the mean Mean precipitation over the study areas increases from north to southarea increases from North to South, with annual precipitation sums between ranging from 500 and to 1100 mm for in the South German Escarpment, around 1000 mm ~~for~~ in the Eastern Mountain Ranges, 1500 and 2500 mm in the Alpine Foreland, and 1000 and 2000 mm in the Alps ~~. However, the valleys of the Inn catchment represent a more arid region with precipitation sums lower than 1000 mm (Poschlod et al., 2020).~~ according to the SDCLIREF observation dataset for the present climate period between 1980 and 2009. The annual mean temperatures are ~~also~~ higher in the North than in the South. The annual mean temperature in the Main catchment, ~~which mainly covers the~~ covering the majority of the South German Escarpment subregion is around 10 °C, whereas in the Alps, the annual mean temperature is around 5 °C. For the regions of the Alpine Foreland and Eastern Mountain Ranges, temperatures vary between 6 and 9 °C, depending on the elevation (Willkofer et al., 2020). The climatology in the study area is influenced by orography (Poschlod et al., 2020)~~. The influence of orography on local conditions is~~ , which could be relevant for wildfire propagation. For example, steep slopes ~~can~~ favour fire spread due to local thermal winds and southern facing slopes show hotter and drier conditions, which increases the risk of fire ignition and propagation (San-Miguel-Ayanz et al., 2018).

2.3 The Canadian Fire Weather Index

In this study, we ~~use~~ used the Canadian Fire Weather Index (FWI) of van Wagner and Pickett (1985) to asses fire ~~risk~~danger, because fire occurrences are strongly related to the FWI ~~(Barbero et al., 2015)~~ (e. g. Barbero et al., 2015) and its global applicability has been demonstrated by several studies (Di Giuseppe et al., 2016; Touma et al., 2021). The Canadian Forest Fire Weather Index System (CFFWIS) ~~constitutes~~ is composed of five sub-indices, which together ~~built~~ build the sixth index, i.e. the final FWI (~~s. figure~~ see Figure 2). The CFFWIS uses meteorological conditions of the atmosphere on the day of interest (temperature, relative humidity, wind speed ~~at noon~~ - all at noon - and 24-h accumulated precipitation) and antecedent weather conditions ~~up to 52 days to~~ represented by fuel moisture codes to estimate fire behaviour and fuel moisture (van Wagner, 1987).

The first three sub-indices represent the fuel moisture codes and ~~can be understood as bookkeeping systems, which increase~~ contain information about antecedent conditions, i.e. they represent increased moisture after rain and reduce moisture for each day of drying. The Fine Fuel Moisture Code (FFMC), Duff Moisture Code (DMC), and Drought Code (DC) model daily changes in the moisture content of three different fuel layers with respect to different time lags (De Rigo et al., 2017): The FFMC ~~rates~~ describes the moisture content of the surface litter (up to 1.2 cm), the DMC accounts for moisture of loosely-compacted organic matter in up to 7 cm depth, and the DC estimates the moisture content of compact, organic layers up to 15 cm of ground depth. ~~According to the~~ The response to immediate atmospheric effects decreases with an increasing layer depth of the specific fuel moisture codes ~~, the response to immediate atmospheric effects decelerates~~ (De Rigo et al., 2017). The fuel moisture codes are considered to dry exponentially over time, so that their immediate drying rate is proportional to the free moisture content. The time lag accounts for the drying speed. DMC and DC respond to changing day length as the season progresses, since less time is available for drying when day length decreases (van Wagner and Pickett, 1985).

The other two sub-indices, i.e. the Build Up Index (BUI) and Initial Spread Index (ISI), together with the resulting FWI, describe the fire behaviour in case of an ignition. They are stateless and ~~without memory of~~ only indirectly linked to past conditions. The ISI combines wind speed and the FFMC to represent the rate of spread~~without the influence of fuel variability~~. The BUI combines DMC and DC to represent the available fuel of the spreading fire. Finally, a combination of ISI and BUI

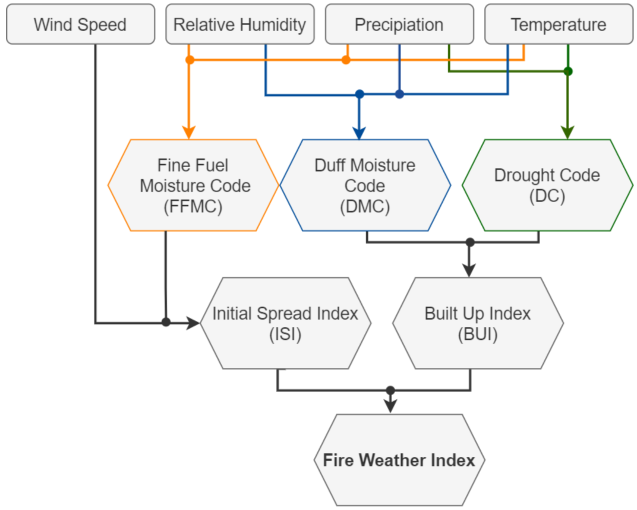

Figure 2. The Canadian Forest Fire Weather Index System, its input variables, and its intermediate indices. Fuel moisture codes (FFMC, DMC and DC) capture the antecedent moisture conditions of the vegetationorganic matter. Fire behaviour codes (ISI, BUI and FWI) describe the potential spread and intensity of the fire (modified , from van Wagner (1987)).

leads to a representation of the potential intensity of the spreading fire in terms of the energy output rate per unit length of fire front, known as the FWI (De Rigo et al., 2017).

Originally, the index was calibrated to pine forest. Pine forest is found almost continuously across FWI was calibrated for pine forests. Pine forests are widespread in Canada, where the index was developed. However, the main goal of the CFFWIS is was to create a fire danger rating system solely based on weather and to provide uniform results throughout Canada. Therefore, the calibration to a specific fuel type can be neglected (van Wagner and Pickett, 1985). The Its applicability to other fuel types in different regions of the world has been demonstrated by various studies (e.g., Di Giuseppe et al., 2016; Barbero et al., 2020; De Rigo et al., (e. g. Di Giuseppe et al., 2016; Barbero et al., 2020; De Rigo et al., 2017; Touma et al., 2021). The full formulas of the CFFWIS and a detailed description of all sub-indices is provided by van Wagner (1987).

2.4 Estimating Fire Danger fire danger using the CRCM5-LE

We calculated daily FWIs for each on a daily basis for each full year (January to December1^{st} to December 31^{st}) and climate model ensemble member between 1980 and 2099 using the CFFDRS R package (Wang et al., 2017). The generated dataset is was later cropped to the fire dry season (April 1^{st} to September 30^{th}) of the northern hemisphere(Vitolo et al., 2019). If not stated otherwise, the , which was used as the fire season in our study as suggested by Vitolo et al. (2019). The results shown refer to this fire season. Subsetting the dataset to the fire season of annually calculated FWI values crops out the spin-up phase of 52-days in the DC. To facilitate the interpretation of the FWI, we use used the seven fire danger classes proposed by the European Forest Fire Information System (EFFIS, 2021) and assign (EFFIS; EFFIS, 2021) and assigned the FWI to particular fire danger levels. These FWI danger levels and their corresponding color mapping scheme are shown in table Table 1.

Table 1. Fire danger levels of the FWI according to EFFIS (2021)

FWI~~range~~	**FWI danger level**	**Color**
< 5.2	No Danger	
5.2 - 11.2	Low	
11.2 - 21.3	Moderate	
21.3 - 38	High	
38 - 50	Very High	
50-70	Extreme	
> 70	Very Extreme	

To ensure that the CRCM5-LE ~~samples~~ sampled the FWI in a meaningful way, we ~~compare~~ compared the CRCM5-LE FWI ~~for the reference~~ median for the current period (1980–2009) ~~to the ERA-5 based FWI dataset of Vitolo et al. (2020), further~~ with the median of the ERA-5-based FWI dataset from Vitolo et al. (2020), hereafter referred to as the "reference dataset" (REF). A majority of the reference data points is located ~~in the blue shaded area, which represents the ensemble's standard deviation for the FWI median of each member (s. figure~~ within one standard deviation of the CRCM5-LE (see Figure 3). The remaining data points are located between the 25th and 75th ~~percentile~~ quantile of the ensemble (blue lines). Overall, the ensemble slightly overestimates the ~~FWI by~~ reference FWI dataset with an average deviation of +0.76~~, but~~ . However, it includes the reference dataset values within its 25th and 75th ~~percentiles.~~quantiles.

The spatial differences between the ~~dataset are fairly low~~ ensemble and reference datasets are fairly small for the Alps and Alpine Foreland in the South (~~s. figure~~ see Figure 4). In the northern ~~parts~~ and especially northwestern parts (~~i. e.~~ i.e. Southgerman Escarpment) of the study area, the CRCM5-LE overestimates FWI values in comparison to the ~~REF dataset on a magnitude between two and~~ reference dataset by an order of two to four. However, ~~this~~ the overestimation in specific regions does not affect ~~the climate change impact assessment of our study, because we compare FWI values solely~~ our analysis, which assesses changes in FWI by comparing FWI derived from the CRCM5-LE for a future and a reference period.

2.5 Changes in ~~Fire Danger~~

2.5.1 ~~Trends~~

~~We evaluate the fire danger trends fire danger~~ We evaluated changes of fire danger derived from the CRCM5-LE over the time period 1980 to 2099 in the study area with statistical metrics: Median ~~conditions are~~ and extreme conditions were examined using the 50th ~~percentile (median)~~ and 90th quantiles of the FWI~~. Extreme conditions are evaluated via the 90th percentile (extreme). The percentiles are~~ , respectively. The quantiles were calculated for different aggregation levels, either temporally ~~, summarizing FWI values of a fire season on daily, monthly or annual basis, or~~ on a monthly scale or spatially for the previously defined subregions. ~~Increasing fire danger is either analyzed continuously from 1980 to 2099 or~~ We derived the median and

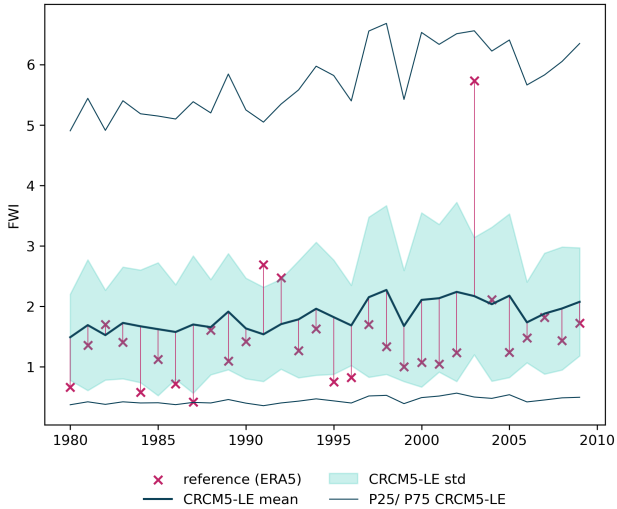

Figure 3. Median FWI ~~for the CRCM5-LE mean~~ (thick blue line) and standard deviation (light blue shading) for the CRCM5-LE mean in comparison to the reference dataset of Vitolo et al. (2020) marked in pink (X for values, lines for deviation from the CRCM5-LE mean). ~~Top~~ The top and bottom blue lines ~~mark~~ represent the 25th and 75th ~~percentile~~ quantiles of the CRCM5-LE, respectively.

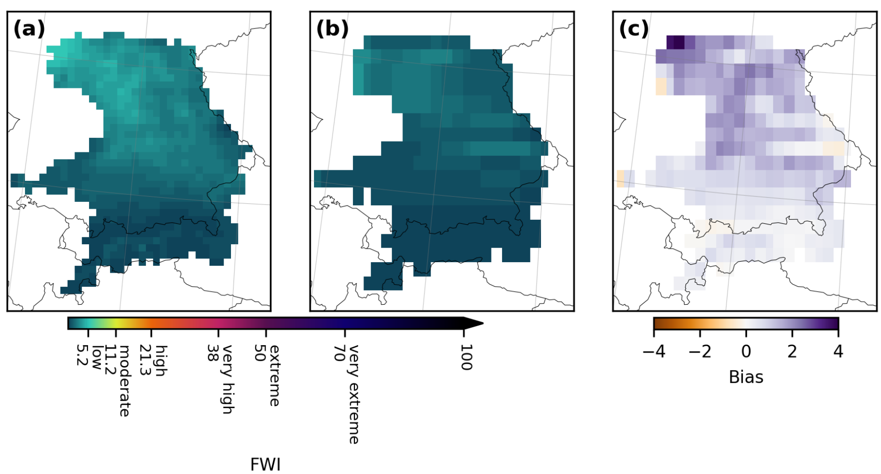

Figure 4. Median FWI of (a) the CRCM5-LE, (b) reference dataset of Vitolo et al. (2020) and (c) difference (CRCM5-LE - reference dataset) for the present time period (1980–2009). The dataset difference ~~is~~ was calculated ~~from~~ by resampling (a) to the spatial resolution of (b) using a nearest neighbour approach.

extreme for each ensemble member separately. Changes of fire danger were either compared between two climate periods ~~.~~ or analyzed continuously from 1980 to 2099. For the climate period comparison, the dataset ~~is~~ was split into two 30-year periods: 1980–2009 ~~as present~~ and 2070–2099 ~~as future~~ representing current and future climate conditions, respectively. For both periods, we derived the median and extreme quantiles for each fire season month for each of the 50 members of the CRCM5-LE. ~~To highlight areas which show~~

2.5.1 Assessing spatio-temporal changes

We used signal maps, which consider the robustness and mangnitude of changes in FWI, to highlight areas with particularly robust and strong changes in the FWI between ~~the climate periods , signal maps are created using the approach of Böhnisch et al. (2021). Signal maps consider the robustness and magnitude of fire danger increases. If the average fire danger~~ climate periods (Böhnisch et al., 2021). The change signal of a grid cell was assumed to be robust if a grid cell's median or extreme fire danger level in the future period ~~is~~ was higher in comparison to ~~the~~ its fire danger level (see Table 1) in the present period for more than 90 % of the climate model ensemble members (45 out of 50)~~, the signal is assumed to be robust. This method is used instead of a statistical test (Böhnisch et al., 2021). We create signal maps for the fire season months representing the median and extreme FWI (s. figure 5) using the FWI danger levels of EFFIS (2021) (s. table 1). Further, we provide~~ .

For the continuous temporal analysis, we provided fire-rings in the style of the warming stripes of Hawkins (2018) to show how the FWI changes over the years on a monthly and subregional scale. The fire rings were derived for each year and all months of the fire season, based on the ensemble mean of the member-specific median or extreme quantile of the FWI for the defined subregions.

2.5.2 Time of ~~Emergence~~emergence

The second part of the climate change impacts analysis ~~focuses~~ focused on the time of emergence (TOE), which ~~is~~ was calculated following the approach of Fargeon et al. (2020): the TOE is reached when a projected metric (~~e. g.~~ e.g. the median of the FWI) crosses the upper bound of ~~the~~ its confidence interval. The confidence interval ~~is~~ was here defined as one standard deviation ~~across the~~ of the distribution of the climate model ensemble members of the present climate period for the mean and extreme quantiles, respectively. The TOE ~~is~~ was defined as the time when the 30-year running ~~average~~ mean trend of the ensemble mean exceeds the confidence interval. To account for the heterogeneous climate conditions in the study area, the TOE ~~is~~ was calculated for each subregion separately. We ~~use~~ used the median and extreme FWI ~~percentiles~~ quantiles of each fire season and ensemble member between 1980 and 2099 for each subregion as the basis for calculating the time of emergence.

2.5.3 Frequency ~~Changes~~changes

~~We assess changes in the fire danger levels of the median and extreme data samples of our dataset by comparing the frequency~~ We assessed fire danger frequency changes in two ways: First, we compared frequency changes of daily fire danger ~~classes for each subregion~~ levels of a fire season between the present and future climate ~~periods (median) and calculating the~~ period for each subregion. Second, we calculated changes in return periods of different FWI ~~extreme thresholds (extreme). To illustrate the median changes of fire danger, we classify the daily values of~~ quantiles corresponding to return periods of 10-, 20-, 50- and 100-years under current climate conditions.

For the first analysis, we classified daily FWI values during the fire season for each member of the CRCM5-LE according to the EFFIS classification ~~in table~~ (Table 1~~(EFFIS, 2021)~~). We show the relative frequency of each fire danger level across the ensemble members for the present and future climate period to highlight fire danger level changes in the four subregions.

~~We determine return periods for different fire danger levels to put the extreme values of the CRCM5-LE in a more tangible context. We calculate~~ For the second analysis, we calculated changes in the return periods ~~on the basis of the 90th, 95th, 98th and 99th percentiles of the present climate period (~~of FWI quantiles that correspond to return periods of 10-, 20-, 50- and 100-years under current climate conditions (period 1980–2009) ~~to account for 10, 20, 50 and 100 year FWI events in~~ for the four subregions. ~~From 2010~~ To do so, we pooled daily FWI values over the entire 50-member ensemble (183 days per fire season x 30 year climate period x 50 members). Using this data pool, we determined the non-exceedance probability p of each FWI value in the present climate period using its rank r and the total sample size n following $p = r/n$. We derived FWI quantiles in the current climate period for non-exceedance probabilities of $p = [0.9, 0.95, 0.98, 0.99]$ and the corresponding FWI return periods T of 10-, 20-, 50-, and 100-years using $T = \mu/(1-p)$, where μ is the inter-arrival time (1/183 days in a fire season) (Coles, 2001). To analyze changes in return periods over time (from 1980 to ~~2099, we create centered~~ 2099), we created centred, rolling 30-year ~~windows of our data sample and determine the FWI percentiles corresponding to the different return periods of the present climate period. The last full~~ windows for each ensemble member (183 days per fire season x 30 year climate period) and derived the cumulative distribution of the time window using the *rv_histogram.cdf* function of the Scipy package in Python (Virtanen et al., 2020). We mapped the FWI quantiles representing the 10-, 20-, 50-, and 100-year return periods of the current period (1980–2009) to future return periods, by deriving their non-exceedance probability p in the cumulative distribution of the rolling window climate period (future). Next, we placed their future probability p into $T = \mu/(1-p)$ (Coles, 2001) to determine the return period T of the present FWI quantile under future climate conditions. This approach allows us to show how the return period of e.g. the current 100-year FWI will change over time with climate change. Due to the centred window approach, the first full 30-year window is 1995 and the last full 30-year window is 2084. ~~For the following years the window size decreases by one element until 2099, with a window size of 15 years. We then compute the non-exceedance probability of the present percentiles given the future cumulative distribution. From the future non-exceedance probability, we estimate the future return periods using the function~~

$$T = 1/(1-p)$$

~~where T is the return period~~ Therefore, we show results between 1995 and ~~p is the non-exceedance probability (Brunner et al., 2021; Coles,).~~ 2084.

3 Results

3.1 ~~Trends~~ Increasing fire danger

~~Fire danger will increase up to a high level for the~~ Under the RCP8.5 emission scenario, fire danger in central Europe will increase (see Figure 5). The FWI median (50th ~~percentile) and up to an extreme level for the FWI extreme~~ quantile) will correspond to moderate and high fire danger levels in some regions and FWI extremes (90^{th} percentile) in the study area quantile) will even reach extreme danger levels by the end of the century (2070–2099)(s. Figure 5). Significant changes for an increase of one fire danger level (thin dot in figure . Significant increases in fire danger levels (thin dots in Figure 5) first occur in June and remain present throughout the study area until September for both the median and extreme FWI. For increases of two fire danger levels, significant changes occur in the months Highlighting grid cells, which experience a rise of at least two levels, helps us to identify regional hotspots of future increases in fire danger. We find increases in fire danger of at least two levels for the Southgerman Escarpment in July and August for the median FWI and for the months July, August and September in August for the extreme FWI(thick dot in figure 5). We distinguish between weaker (one level, thin dots) and stronger (two levels, thick dots) fire danger level rises, because in July and August almost the entire study area shows a robust fire danger level rise of one level for both median and extreme conditions. This helps us to identify regional hotspots. The Southgerman Escarpment in . The other subregions (Alps, Alpine Foreland, Eastern Mountain Ranges) are affected by a two-level rise in danger-level of the extreme FWI in August. Additionally, the western parts of the Southgerman Escarpment and parts of the northwest is most affected by changes in the median FWI while the Alps and the Eastern Mountain Ranges experience the strongest fire danger level rises in are affected by a two-level danger-level increase in September for the extreme FWI in the months July to September (s. figure (see Figure 5).

Increases in fire danger are visible throughout Mai to September and particularly pronounced from July to September , but are also visible throughout Mai to September (s. figure (see Figure 6). The median case FWI points out that high fire danger becomes the average condition in the Alpine Foreland by 2080, in the Southgerman Escarpment by 2060 and in the Eastern Mountain Ranges by 2070 (s. figure see Figure 6 [1]). The Alps are exposed to high fire danger only in the extreme case (s. figure when looking at the extreme FWI from 2070 onwards (see Figure 6 [2])from 2070 onwards. The other subregions are much more strongly affected by changes in the extreme caseFWI than the Alps: Very high and high fire danger occur frequently in July and August in the second half of the 21^{st} century in the Alpine Foreland and Eastern Mountain Ranges for the extreme FWI. In the Southgerman Escarpment, this is the case in June and September. However, for For July and August, very high fire and high danger and almost extreme fire danger levels occur frequently from 2030 onwards (s. figure 6). The ensemble mean shows hardly any fire danger changes over the 21^{st} century in the median and extreme case for April (s. figure in the extreme FWI in the Southgerman Escarpment (see Figure 6). High fire danger becomes the mean condition (median) median condition in the summer months towards the end of the century for large parts of the study region (figures see Figures 5 and 6).

3.2 Time of Emergenceemergence

The results for the TOE show that the climate change signal exceeds the natural variability before the middle of the 21internal variability in all sub-regions by mid-21^{st} century in all subregions for both median and extreme FWI (s. figure see Figure 7). For all subregions, except the Alpine Foreland, the TOE is reached in the same year for both the median and the extreme FWI. The earliest TOE is reached in the Alps in 2032, followed by the Alpine Foreland in 2039 for the median and in 2041 for the extreme FWI. In the Southgerman Escarpment, the TOE is reached in 2044 and in the Eastern Mountain Ranges in

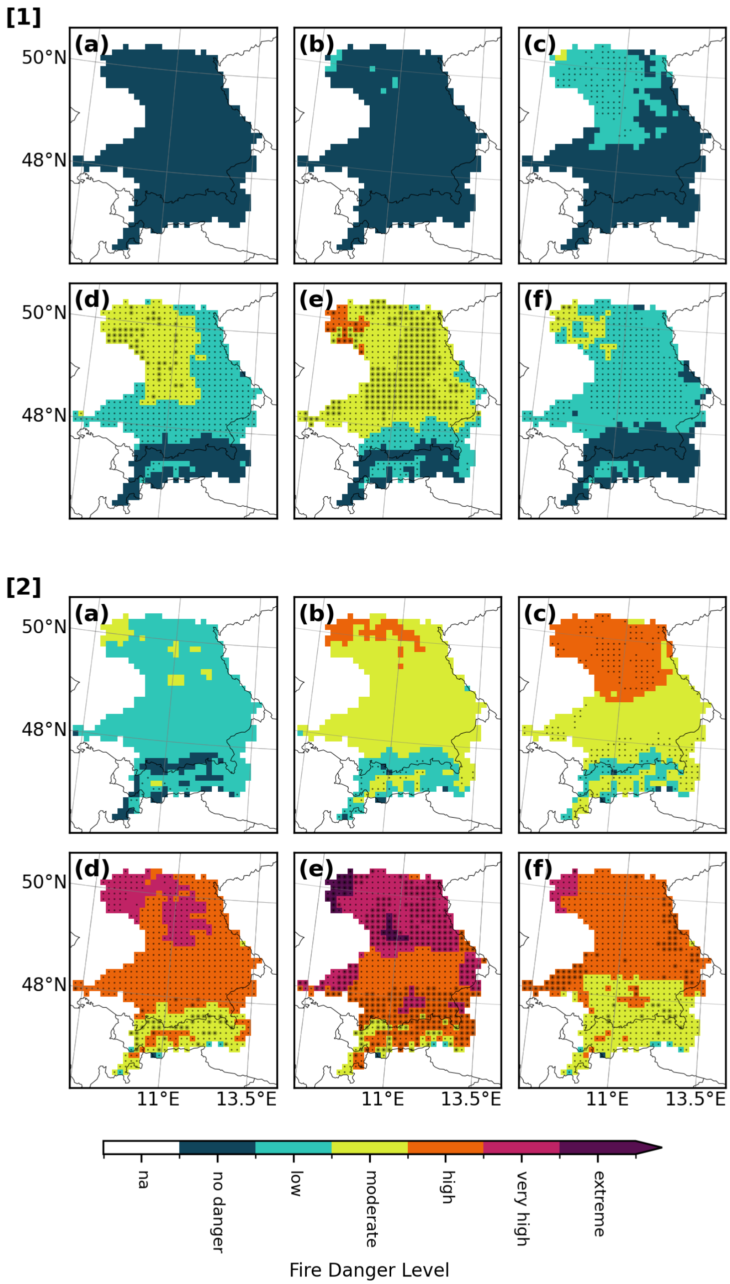

Figure 5. Ensemble mean of the median ([1], 50th ~~percentile~~quantile) and extreme FWI ([2], 90th ~~percentile~~quantile) by fire season month (April (a) - September (f)) for the future time period 2070–2099. Dots indicate that 90% of the CRCM5-LE members agree on a fire danger level increase of at least one level (thin black dots) or at least two (thick black dots) levels compared to the present period (1980–2009).

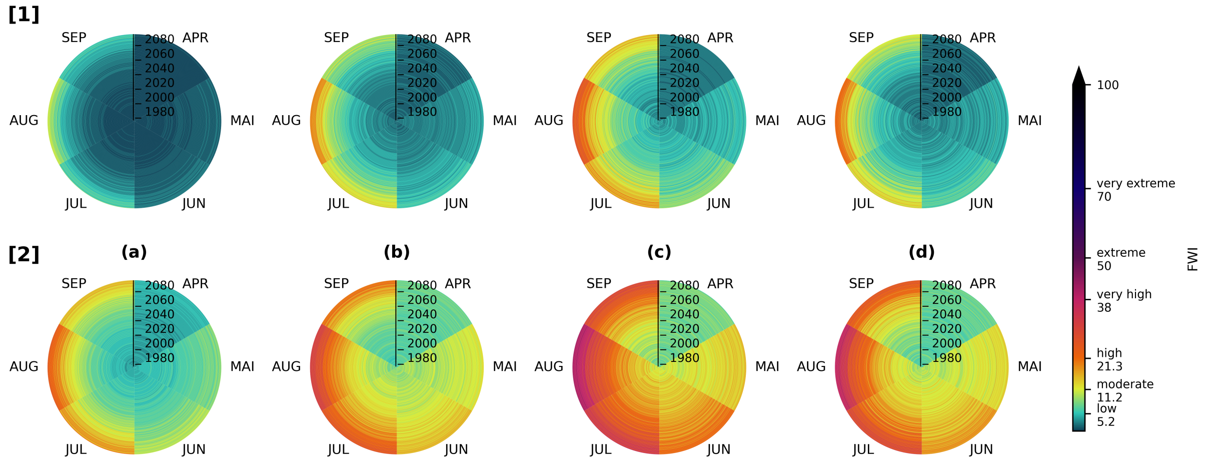

Figure 6. Fire rings show the FWI of the ensemble mean of the monthly median ([1], 50th ~~percentile~~quantile) and extreme ([2], 90th ~~percentile~~quantile) ~~FWI~~ of each subregion (Alps, Alpine Foreland, Southgerman Escarpment and Eastern Mountain Ranges (a-d)) during the fire season (April - September) between 1980 and ~~2099~~2099.

2047 for both the median and the extreme FWI. ~~This finding indicates that the distribution of the FWI extremes resembles the distribution of the FWI median.~~

FWI ~~changes~~ increases in the Alps are weaker than in the other subregions. Still, the TOE is reached quite early in this region because the FWI and its variability are very low in the present climate period. Throughout the 21st century, the median and extreme FWI ~~increase strongly~~will increase continuously in the Alps. While the extreme FWI is projected to shift from low to moderate fire danger in this subregion, the median FWI shows hardly any changes and remains in the no danger level ~~(below five)according to EFFIS (2021).~~

zone even at the end of the century (see Table 1). For the other subregions, the median of the fire season is currently low but increases towards a moderate danger level in the future. ~~In the extreme case, the average~~ For the extreme FWI, the ensemble mean fire danger is moderate (11.2 < moderate ~~>~~ < 21.3, ~~s. table~~ see Table 1) in the present, but increases until the end of the century up to a high level (21.3 < high ~~>~~ < 38, ~~s. table~~ see Table 1) with values greater than 30 for the Southgerman Escarpment, slightly smaller than 30 for the Eastern Mountain Ranges and approximately 25 in the Alpine Foreland (~~figure~~ Figure 7). In general, increases in fire danger in the extreme FWI are of such a magnitude that the lower bounds of the ensemble standard deviation ~~exceeds~~ exceed the upper bounds of the standard deviation of the present climate period for all subregions by the end of the 21st century.

3.3 Increasing ~~Frequency~~ frequency of ~~Extreme Events~~extreme events

In the future (2070–2099), the percentage of days with fire danger (>= low) ~~shift from one out of ten to one out of three days~~ shifts from 10 % to 33% in the Alps, ~~one third to half~~ from 25% to 50% in the Alpine Foreland and ~~Eastern Mountain Ranges,~~

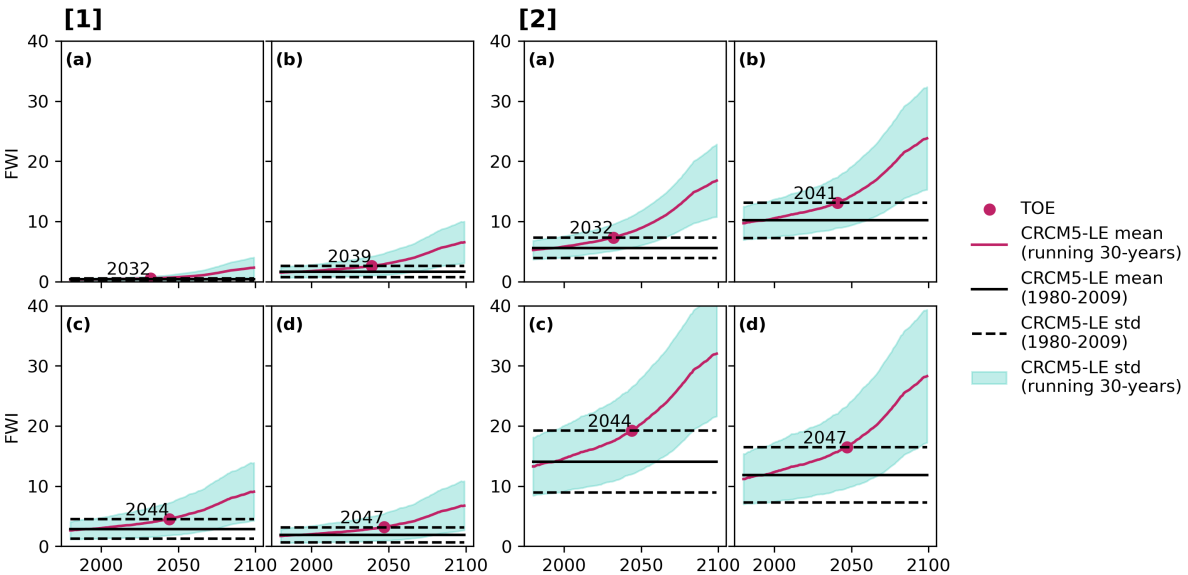

Figure 7. ~~Trends~~ Increases of the median ([1], 50th ~~percentile~~quantile) and extreme ([2], 90th ~~percentile~~quantile) FWI between 1980 and 2099 differentiated by subregion: (a) Alps, (b) Alpine Foreland, (c) Southgerman Escarpment, (d) Eastern Mountain Ranges. The ensemble mean ~~trend~~ increase is derived on a fire season basis and represented by solid pink lines smoothed over a 30-year window. The ensemble's standard deviation is represented by shaded blue areas. Black solid and dashed lines represent the ensemble mean and spread of the present climate period (1980–2009). The TOE, marked with a pink dot and year annotation, is reached when the ensemble mean (pink line) crosses the upper boundary of the ensemble standard deviation in the present climate period (black dashed line).

~~and one third to less than half in the Southgerman Escarpment (s. figure~~ Southgerman Escarpment, and from 33% to 60% in the Eastern Mountain Ranges (see Figure 8). In the Alps, no and low fire danger days ~~represent~~ currently account for 182 out of 183 days (99 %) of the fire season~~in the present~~. In the future, ~~this will drop~~ the number of such days will decrease to approximately 160 ~~days of the~~ out of 183 ~~day long fire season~~days (87 %). In the Alpine Foreland ~~,~~ and Southgerman Escarpment, the number of days with moderate, high, and very high fire danger ~~occur during one third of the days in the futurefire season~~increases by 15% from the present to the future. The high and very high ~~class~~ danger level classes are not observed in the present climate period, but ~~occur~~ emerge in the future ~~. In the Eastern Mountain Ranges, similar results are observed: While the higher danger levels already occur in the present, very high danger levels additionally~~ in the Alpine Foreland and the Southgerman Escarpment. The difference between these two regions lies in the proportions of very high and extreme fire danger days, which are more likely to occur in the Southgerman Escarpment (4%) than in the Alpine Foreland (1%) in the future. In ~~comparison to the Alpine Foreland, moderate~~ the Eastern Mountain ranges, the frequency of low (20%) and moderate (15 %) fire danger days ~~are less frequent and high~~ in the future is similar to the Southgerman Escarpment and the Alpine Foreland. Our results show differences in the frequencies of high, very high and extreme fire danger days ~~are more frequent in~~ between the Eastern

Mountain Ranges and the other subregions. In the Eastern Mountain Ranges, the very high fire danger level is most common among all regions in the future and days with high fire danger increase from 4% in the present to 15 % in the future. As in the other subregions, very high and extreme fire danger days do not occur in the present but are observed during 5% of the days in the future. ~~For the Southgerman Escarpment, changes from present to future resemble those in the Eastern Mountain Ranges with the difference that the high and very high class are represented more frequently.~~

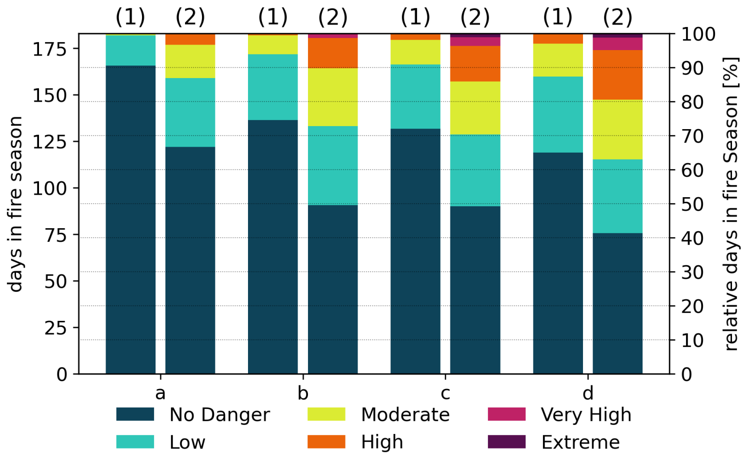

Figure 8. ~~Frequency~~ Number of days experiencing specific fire danger levels ~~in~~ during the fire season (April – September, 183 days) for the present (1; 1980–2009) and future (2; 2070–2099) climate period. FWI danger classes ~~are~~ were derived for the subregions (a) Alps, (b) Alpine Foreland, (c) Southgerman Escarpment and (d) Eastern Mountain Ranges.

~~In all subregions, the frequency of distinct FWI extremes increases towards the end of the 21st century (figure 9). The frequency of~~ The return periods of current-climate 100-, 50-, 20- and ~~10-year FWI extremes at least doubles until~~ 10-yearly FWI extremes will at least halve by the end of the 21st century in all subregions (~~s. figure (~~see Figure 9). Generally, the results for the four subregions are quite similar and vary only slightly in ~~details~~detail. In all subregions, the ~~return period of the~~ present 100-year event will become the 50-year event in the early ~~2030ies~~2030s, the 20-year event in the ~~2060ies and the ten year~~ 2060s and the 10-year event by 2090. The 10-year events of the present will occur every five years by 2060 and every three years by 2090.

~~Surprisingly, the~~ The spread of the return periods decreases in the future, indicating a stronger increase in the frequency of very extreme events (i.e. 100- and 50- year events) than for mid-range extreme events (i.e. 20- and 10-year events) ~~. This finding is depicted by the increasing density and overlapping ensemble realisations for different return periods towards the end of the century. For example, the 100-year event of the Eastern Mountain Ranges becomes a 10-year event by 2090. If the increase of extreme events was proportional, we would expect the 10-year event to become a 1-year event at approximately the same time. This is not the case. Instead, the 10-year event becomes a 3-year event by 2090 in the Eastern Mountain Ranges, implying changes in the FWI value distribution over time (s. figure~~ (see Figure 9).

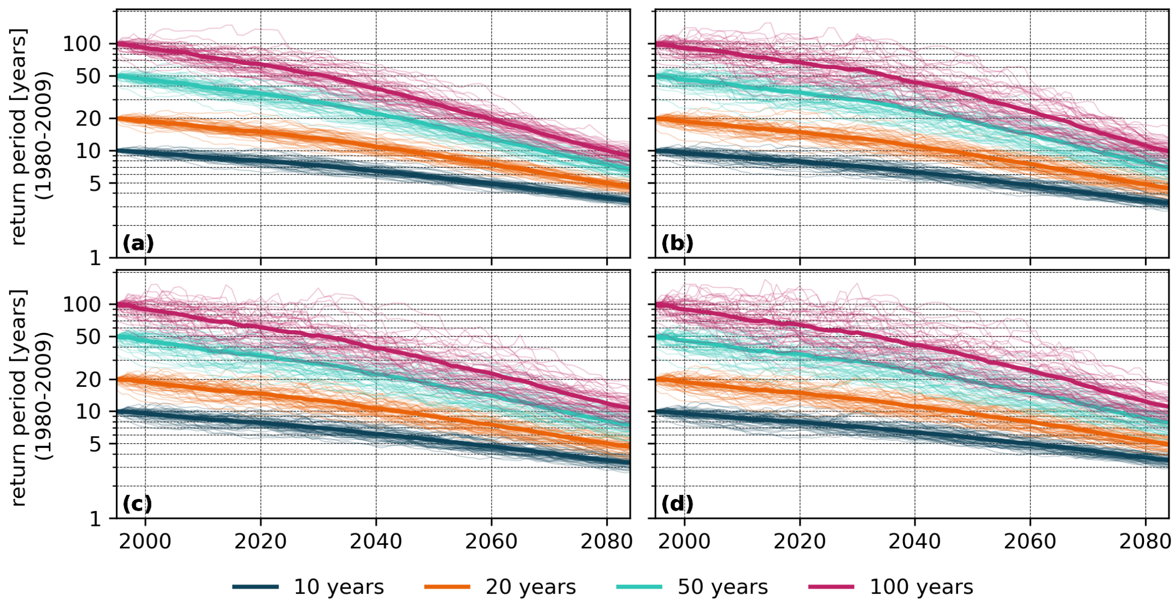

Figure 9. ~~Changes~~ Future changes (1995–2084) in ~~current~~ the return periods ~~(1980–2009)~~ of ~~the 90th~~FWI-quantiles corresponding to return periods of 10-, ~~95th~~20-, ~~98th~~ 50- and ~~99th FWI percentile throughout the 21st century~~ 100-years under current climate conditions (~~2010–2099~~1980–2009) ~~, distinguished by subregion~~for the four subregions: (a) Alps, (b) Alpine Foreland, (c) Southgerman Escarpment, (d) Eastern Mountain Ranges. The thick solid line represents the CRCM5-LE mean, while thin lines represent the 50 ensemble members.

4 Discussion

4.1 Spatio-temporal trends and variability

Our results demonstrate that fire danger ~~increases dramatically over the next few decades in Central Europe . The trend towards hazardous fire danger conditions in the future~~ in central Europe increases strongly until the end of the 21st century, if the RCP8.5 scenario is assumed. The future increase of the number of days with conditions favoring high or higher levels of fire danger emerges for all ~~presented metrics~~ metrics assessed in this study, i.e. different ~~temporal, spatial and ensemble aggregation levels . First, the discussion highlights the relevant characteristics of the dataset used in this study. Second, we examine the limitations~~ quantiles and aggregation levels of the ~~FWI and~~ ensemble and in space and time. Within the ensemble spread, increases in fire danger extremes (90th quantile) are more pronounced than increases in median (50th quantile) conditions according to all assessed metrics (see Figures 5, 6 and 8). In space, we find that the variability of the FWI increases more strongly in mountain regions than in non-mountain regions, which is demonstrated by smaller changes in the median FWI than in the extreme FWI in the Alps and smaller differences in the increases in median and extreme fire danger for less complex terrain (Alpine Foreland and Southgerman Escarpment) (see Figure 5). This corroborates findings by Wastl et al. (2012), who explained the higher fire danger ~~levels. Third, we discuss the results in a spatio-temporal context with a special focus on fire danger~~ variability ~~. Last,~~

we elaborate on the societal and ecologic implications of our findings. in mountain regions by the higher terrain variability, i.e. rain-shadow effects and katabatic dry winds (Foehn). In time, extreme fire weather (90^{th} quantile) is more likely to occur in the second half than in the first half of the fire season because the differences between the median and extreme FWI quantiles are smaller in April, May and June, than in July, August and September (see Figure 5).

4.2 Data Basis

Before starting our analysis, we compared the results from the CRCM5-LE to Our results for the TOE and the projected FWI in all subregions except the Alps are similar to the findings of Fargeon et al. (2020) for France, where TOE is reached for both quantiles (50^{th} and 90^{th}) around 2060 (Fargeon et al., 2020), i.e. about 20 years later than in HydBav (see Figure 7). Reasons for this delay in TOE in France could be because of the later and shorter reference period (1995–2015) used by Fargeon et al. (2020), the dataset of Vitolo et al. (2020) for the present climate period (1980–2009). The larger uncertainty range originating from natural variability and model uncertainty in the multi-model ensemble as compared to the SMILE (Deser et al., 2012), the warmer and drier climate change signal of the CRCM5-LE slightly exceeds the FWI in comparison to the reference dataset (s. figure 3) , especially in the northwestern parts of the study area (s. figure 4). The runs with the CRCM5-LE are generated using the CFFDRS R package, whereas the reference dataset from Vitolo et al. (2020) uses the Global ECMWF Fire Forecast (GEFF) model (Di Giuseppe et al., 2016). These models differ slightly in their results, since the GEFF model applies the original FWI formulas from van Wagner and Pickett (1985), while Wang et al. (2017) adjusted the formulas for DC and DMC in the CFFDRS R-package (Vitolo et al., 2019). Nevertheless, the validation set-up demonstrates that the implemented algorithm generates meaningful results(von Trentini et al., 2019), or differences in the climate of the study regions. While Fargeon et al. (2020) point out that fire danger increases are hard to distinguish from internal variability in northern France when using a multi-model ensemble, we demonstrate that increases in fire danger can robustly be quantified for central Europe when using a regional SMILE.

Another aspect, which has to be discussed, is the strong tiling pattern visible in figure 5 2in the months June and August. This tiling pattern is already visible in the extreme values of the input variables. We provide a sensitivity analysis of the FWI in the Appendix (s. figure A3) , where the tiling occurs for temperature and relative humidity in the 95^{th} percentile as well. The pattern correlates with invariate fields from the geophysical baseline parameterisation

4.2 Dataset specific uncertainties

Though SMILEs can account for internal variability, they are not designed to evaluate the structural uncertainty of the climate models (Deser et al., 2020). Structural or model uncertainty can only be assessed in multi-model studies (i.e. Fargeon et al., 2020) . In order to quantify both – internal variability and structural uncertainty – it would be necessary to use multiple SMILEs as provided by the "Multi-Model Large Ensemble Archive" (MMLEA; Deser et al., 2020). However, all SMILEs in the MMLEA are based on Global Climate Models (GCMs) with a spatial resolution ranging between 2.8° and 0.9° (Deser et al., 2020). On a regional and local scale, a higher spatial resolution is needed to quantify climate change impacts on forest fires. For Europe, only two other dynamically downscaled SMILEs from Regional Climate Models (RCMs) exist besides the CRCM5-LE: The

16-member EC-EARTH-RACMO ensemble at 0.11° (Aalbers et al., 2018) and the 21-member CESM-CCLM ensemble at 0.44° grid cell size (Brönnimann et al., 2018; Fischer et al., 2013). The models differ in their study domain (EC-EARTH-RACMO) and spatial resolution (CESM-CCLM) from the CRCM5-LE used here (Wood, 2023; von Trentini et al., 2020).

The CRCM5 represents FWI at much finer spatial resolution than CanESM2 and therefore adds robust high-resolution features (Böhnisch et al., 2020). However, we find tiling patterns on the border between the Southgerman Escarpment and the Alpine Foreland (see Figure 5), which correspond to the geophysical baseline parameterization of the CanESM2 ~~, e.g. bedrock depth. Over the areas where the strong tiling occurs, bedrock depth is about 5m. The water storage potential of the ground is especially high in this area compared to its surrounding areas with an average bedrock depth between 1 or 2 meters. Such high storage potential can affect evaporation and leads to a higher cooling in areas with high bedrock depths which results in lower temperatures and higher relative humidity~~(see Figure A4). In comparison to the CORDEX multi-model ensemble, the CRCM5-LE shows drier and warmer climate change signals for temperature and precipitation (von Trentini et al., 2019) . These characteristics of the CRCM5-LE are in line with the results from the validation (see Figure 3) and suggest that our results represent an upper limit of the expected changes in future fire danger.

~~Lastly, the SMILE used in this study assesses climate change signals against internal climate variability but does not consider uncertainties related to emission scenarios and the chosen climate model. However, the choice of emissions scenarios also introduces uncertainty. Fire danger increase is projected and analyzed only for the RCP8.5 scenario, which represents the strongest temperature increase scenario. It remains open and subject to policy making if this scenario becomes reality. Arnell et al. (2021) find that reducing emissions to a level consistent with an increase of a global mean temperature of 2°C, i.e. RCP 2.6, reduces fire danger substantially compared to RCP8.5. This finding implies that our change estimates represent an upper boundary of changes in fire danger expected in the future.~~

4.3 ~~FWI and Fire Danger Levels~~

~~In this study,~~ Correcting the bias between climate model data and observation data is often an inevitable step in climate impact studies (Piani et al., 2010). The CRCM5-LE was bias adjusted using univariate quantile mapping (Poschlod et al., 2020; Mpelasoka and Ch . Such univariate methods can change the co-variation between multiple variables (Zscheischler et al., 2019) with potential impacts on the analysis of complex indices like the FWI. Therefore, there have been calls for the use of multi-variate bias correction methods (Cannon, 2018). However, Yang et al. (2015) showed that univariate bias correction was sufficient to study fire weather changes in Sweden. Furthermore, multivariate bias correction is a non-trivial task and fixing co-variation issues between variables might lead to other problems, e.g. with the representation of temporal or spatial dependencies (Vrac, 2018) . In this regard, we assume that the univariate bias correction applied on the ~~statements on extremes are solely based on the percentile thresholds (e. g. 90^{th} percentile for extremes) rather than on individual extreme events. The generalization of the daily calculated FWI to long-term ensemble averages of single months cancels out single extreme events on a sub-monthly scale. Because the FWI is an indicator which identifies and rates dangerous conditions for fire events rather than predicts fire occurrences (Di Giuseppe et al., 2016), aggregation does not limit our findings but eliminates outliers of locally small or temporarily short but very extreme FWI values (FWI > 70)~~CRCM5-LE is appropriate for our analysis.

4.3 Limitations of fire danger metrics

Our validation set-up demonstrates that the algorithm used to compute the FWI generates comparable results to the reference dataset (see Figure 3) even though our analysis used the CFFDRS R package to calculate the FWI (Wang et al., 2017), whereas the reference dataset was generated with the Global ECMWF Fire Forecast (GEFF) model (Di Giuseppe et al., 2016). These models differ slightly in their results because the GEFF model applies the original FWI formulas from van Wagner and Pickett (1985) and the CFFDRS R-package uses adjusted formulas for DC and DMC (Wang et al., 2017).

The FWI used in this study cannot be analysed in terms of events (Wotton, 2009), similar to other indices like the Percent of Normal Index for drought events (Böhnisch et al., 2021). Fires start only in case of an ignition and the FWI as a danger rating index quantifies the ease of ignition, rate of spread and difficulty to control a potential fire (De Rigo et al., 2017). The FWI cannot be analysed in terms of events, similar to other indices like the Percent of Normal Index for drought events (Böhnisch et al., 2021). It rather describes the potential for Therefore, the FWIdescribes fire weather development and is therefore rather than actual event occurrence and is suitable to assess future changes in fire danger (Di Giuseppe et al., 2016).

Further, the classification into danger levels proposed by EFFIS (2021) needs to be critically reflected upon: The FWI consists of four input variables, which implies multivariate inter-dependencies that lead to a high internal variability of the index itself. Parts of our results are based on the EFFIS fire danger levels for the FWI (s. figure 8). First, class memberships are not linearly distributed over the index values within this classification scheme. For example, a FWI increase of 15 between a FWI of 10 and 25 rises the class membership from low to high and covers two classes, whereas the same difference between a FWI of 25 and 40 increases the fire danger level from high to very high. Second, the FWI itself is a complexscheme with exponential, rather than linear relationships (s. Drought Codes of the FWI; van Wagner, 1987). Therefore, using classified values to identify a robust signal normalizes the scale and offers a more interpretable approach to assess increases in fire danger. The CRCM5-LE helped us to show that the increase in fire danger is significant thanks to the ensemble agreement on the observed increases in fire danger classes.

While the FWI addresses fire danger in a meteorological context, it does not account for FWI addresses fire danger in a meteorological context, it does not account for the flammability of the flammability of the surfacesurface. Land-use in our study area is complex, but contiguous forests are present in all four subregions, especially the Eastern Mountain Ranges and the Alps. Persistent snow cover in winter prevents fire occurrences in spring in the Alps (Conedera et al., 2018) and other regions of high elevation, even though fire weather conditions might be met. Large parts of the South German Escarpment and Alpine Foreland are used for agricultural purposes, where fires can spread fast under dry conditions (see Figure A1). However, these regions are more densely populated than the other two regions (Eastern Mountain Ranges and the Alps), which enables a faster suppression of fire incidents. For large-scale FWI analyses, non-burnable areas such as deserts and bare soil are masked out (Vitolo et al., 2020; Touma et al., 2021). However, in (Touma et al., 2021; Vitolo et al., 2020). In the context of the study area HydBav and the 11-km resolution of the CRCM5-LE, land use is was highly variable on a sub-pixel scale and non-burnable areas (e. g. lakes, snow and ice covered areas and urban areas) are therefore not masked out in this study (s. figure (see Figure A1).

4.4 ~~Spatio-Temporal Trends~~ Increasing fire danger and ~~Variability~~implications

~~We find that the region affected most strongly by FWI increases is the northwest, i. e. the Southgerman Escarpment (s. figures 5, 6 and 8). Noteworthy is, that average changes (median) are smaller in the Alps, but increases in the extreme FWI are strongest in the Alps. The trends of the median are similar for the Alpine Foreland and the Eastern Mountain Ranges, but FWI extremes in the Eastern Mountain Ranges increase more strongly than in the Alpine Foreland. We summarize that increases in fire danger extremes are more pronounced than increases in median conditions and therefore variability increases in regions with heterogeneous terrain (Alps and Eastern Mountain Ranges). For less complex terrain (Alpine Foreland and Southgerman Escarpment), the increases in fire danger extremes are less variable. These findings corroborate findings by Wastl et al. (2012), who explained the higher fire danger variability in mountain regions by the higher terrain variability, i.e. rain-shadow effects and katabatic dry winds (foehn).~~

~~Comparing the median and extreme conditions, derived from the 50^th^ and 90^th^ percentile gives insights into the dataset's variability and can differ by the chosen aggregation level, e. g. monthly or daily values. The differences between the percentiles are smaller for April, May and June, than for July, August and September (figure 5). This finding indicates that the seasonal variability is higher for the last three months of the fire season and implies that the probability for extreme FWI conditions is elevated during these late summer months. The ring plots in figure 6 confirm this assumption for the defined subregions. This subregional analysis confirms the Southgerman Escarpment as the~~ We identified the Southgerman Escarpment as a hotspot for dangerous FWI conditions within Hydrological Bavaria ~~. Nevertheless~~(see Figures 5 and 6). However, the other subregions are subject to ~~tremendous changes as well. Especially the months~~ substantial changes in fire danger as well, especially in August and July~~can be identified as seasonal hotspots throughout the study area~~. On average (median), the fire danger will be high in the Alpine Foreland, Southgerman Escarpment and Eastern Mountain Ranges and moderate in the Alps by the end of the century. ~~For the extreme FWI events, such high levels can already be observed by the middle of the century (figure 6).~~ In the Alps, the median FWI does not reach as high fire danger levels as the one in the other subregions because of their elevation-dependent colder climate. Nevertheless, this region is very sensitive to climate change induced fire weather changes as demonstrated by its early TOE (see Figure 7) and its significant danger level changes in the months of July and August (see Figure 5).

~~The question arises whether the fire season considered in this study is too short, when looking at the differences between median and extreme FWI results in the signal maps (figure 5), and the strong increase of the FWI in September in the ring plots (figure 6). According to the results demonstrated in the ring plots (figure 6)~~Over the course of the 21^st^ century, the fire season ~~in HydBav starts in May, when the first dangerous FWI conditions (moderate fire risk) are reached for the extreme FWI sample. In the future, the fire~~ will prolong, as fire danger levels are still elevated ~~and no longer on a no-danger level as in April for the median. This finding~~ in September from 2030 onwards (see Figure 6). This suggests that the fire season ~~length increases~~ might extend to at least October towards the end of the century. For the Southern Alps, Wastl et al. (2012) identified the main fire season between December and April because of low precipitation and ~~missing vegetation cover in the winter half year. Therefore, future~~ decreased fuel moisture outside of the vegetation period (Conedera et al., 2018). Future studies assessing changes in fire danger ~~in the Alps should focus on~~ and fire events in temperate climate regions should therefore consider the whole year instead of the ~~summer~~ vegetation season only.

~~Additionally, we want to highlight the special characteristics of the Alps which are characterized by very complex terrain. Due to their elevation-dependent colder climate, the mean FWI does not reach as dramatic values as in the other subregions. Nevertheless, this region is very sensitive to climate change induced fire weather changes as demonstrated by its early TOE (s. figure 7) and its significant danger level changes in the months July and August (s. figure 5). In the Alps, TOE is reached strikingly earlier than in the other subregions, mainly because of small natural variability in the present climate period. This small variability occurs because there exists currently no fire danger on this high data aggregation level in this specific subregion.~~

~~Besides the low variability of the FWI in the Alps, resulting in a very early TOE, we want to point out that our results for the TOE and the projected FWI in the other subregions are similar to findings for France (Fargeon et al., 2020). Fargeon et al. (2020) found FWI increases between two and twelve index values for the median (50th percentile) and from 15 to 22 index values for the extreme FWI (90th percentile) using a multi-model ensemble under the RCP8.5 scenario over France. TOE is reached in both percentiles around 2060, which is about 20 years later than observed in the results of this study for HydBav. Reasons for this delay could be due to the later and shorter reference period (1995–2015), the overestimation of natural variability in the multi-model ensemble (Fargeon et al., 2020) or the slight overestimation of the CRCM5-LE (s. chapter 2.4). The CRCM5-LE used in our study embodies a substantially larger database than the database used by Fargeon et al. (2020) thanks to its SMILE-setup, which helps to better represent natural variability. While Fargeon et al. (2020) point out that fire danger increases are hard to distinguish from natural variability in northern France in multi-model ensembles, we demonstrate using a SMILE that increases in fire danger are robust for Central Europe.~~

4.5 ~~Societal and Ecologic Impacts~~

Our results highlight the increasing frequency of currently anomalously extreme fire weather that will affect the ~~study regions' fire regime as well~~fire regime of the study region (see Figure 6). Prolonged droughts and exacerbating heat events ~~may~~ might limit fuel availability and therefore fire activity in more arid regions, such as the Mediterranean~~(Bowman et al., 2020; Pausas and Paula, 201~~ ~~. However, for~~ , in the future (Bowman et al., 2020; Pausas and Paula, 2012). For wetter, more productive regions~~and seasons, i.e.~~ , like our study area~~in Central Europe~~, aridity does not limit fuel availability~~, which implies higher sensitivity to flammable conditions (e.g., after hot and dry seasons) and points out the importance of considering vegetation and fuel structure changes in further studies (Pausas and Paula, 2012; Turco et al., 2018). Further, Bowman et al. (2020) suggest that~~ . Bowman et al. (2020) suggested that a declining snow cover in spring and drier fuels in summer will increase burned area in mountain forests, as present in the Alps and Eastern Mountain Ranges~~in our study area.~~ . This implies a higher sensitivity to flammable conditions (e.g., after hot and dry seasons) and an extension of fire events to more northern latitudes and higher elevations.

~~For the Mediterranean, Turco et al. (2018) expect changes in meteorological fire weather~~ Expected changes in fire weather in the Mediterranean are of such a magnitude ~~,~~ that current fire suppression measures ~~are not sufficient anymore. The guidelines for forest fire defence in the federal state of Bavaria currently only ask the public for cautious behaviour when fire danger~~

is elevated. In case of high or very high fire danger, surveillance flights are carried out in the respective areas (?). Studies in might not be sufficient anymore (Turco et al., 2018). Studies for other regions, i.e. e.g. the UK (Arnell et al., 2021) and France (Fargeon et al., 2020), suggest suggested that increases in fire danger should be considered in emergency, land use and management planning to mitigate future fire risk. Taking the results of our study into account, these suggestions apply for Hydrological Bavaria danger. Our research findings indicate that forest fire mitigation measures must be proposed for central Europe and its mountain regions as well.

5 ConclusionConclusions

This study presents the first regional Single Model Initial-Condition Large Ensemble (SMILE) assessment of fire danger increase for Central changes for central Europe, more specifically, the study area Hydrological Bavaria (HydBav). The To date, the study area is not yet irregularly affected by wildfires and high fire danger to date, but will be affected occurs only under very rare conditions (90th FWI quantile). However, high fire danger will become more frequent in the future when assuming an RCP8.5 emission scenarioand accounting for natural variability. The strongest increases and most hazardous developments are observed North Our results demonstrate that fire danger increases substantially throughout the study area during this century. We find the strongest changes and highest fire danger levels north of the river Danube in the summer months of July and August for the subregions South German Escarpment and Eastern Mountain Ranges. Regions south of the Danube (Alps and Alpine Foreland), are less strongly affected by changes in the FWI but increases are still significant. Further, we find that the FWI has a stronger variability for regions with heterogeneous terrain (i.e. the Alps and the Eastern Mountain Ranges) than for regions with less complex terrain (i. e. Alpine Foreland and Southgerman Escarpment). The Our results also show that the time of emergence (TOE) is reached in all subregions of the study area before 2050 and the return period of a present before 2050. Moreover, they show that not only the mean, but also the lowest range of the running mean, indicated by the CRCM5-LEs standard deviation, exceeds the upper limits of the current climate standard deviation (1980-2009) in all subregions before 2099 for the 90th FWI quantile. Last, our findings demonstrate that the return periods of present-climate 100-year event shifts towards a FWI events shift towards 10-year event by 2090. We accept all of our three hypotheses, stated in the introduction (chapter 1). Our results reveal more serious developments than assumed in the original hypotheses.

events by 2090 and the return periods of present-climate 100-, 50- and 20-year events shift to 50-, 20- and 10-year events, respectively, before 2050 for all subregions. This study highlights Our findings highlight future fire danger increases for Central Europe, as central Europe, – an example region with currently moderate to low low to moderate fire danger conditions . Our findings – and stress the importance of developing fire suppression measures to mitigate future fire risk also adapt to these increases in regions with temperate climate.

Data availability. The datasets used in this study can be found in the following repositories: CRCM5-LE: https://www.climex-project.org/de/datenzugang, ERA-5 based FWI: DOI: 10.24381/cds.0e89c522 (31.01.2023), sub-regional division: https://www.lfu.bayern.de/natur/

naturraeume/index.htm, landcover data from Copernicus Land Monitoring Service: https://land.copernicus.eu/pan-european/corine-land-cover/clc2018.

Author contributions. JM, AB, RL and MIB contributed to the conception of the study. JM conducted the data collection for the FWI, statistical analyses and wrote the first version of the manuscript. AB, RL and MIB monitored and supported the research process and revised and edited the manuscript. RL is founder and head of the ClimEx project. All authors contributed to the article and approved the submitted version.

Competing interests. The contact author has declared that neither of the authors has any competing interests.

Acknowledgements. This research was conducted within the ClimEx project (https://www.climex-project.org/), funded by the Bavarian State Ministry for the Environment and Consumer Protection (Grant No. 81-0270-024570/2015) and the FoFix project funded by ETH. CRCM5 was developed by the ESCER Centre of Université du Québec ‘a Montréal (UQAM; https:// escer.uqam.ca/) in collaboration with Environment and Climate Change Canada. Computations with the CRCM5 for the ClimEx project were performed on the HPC system SuperMUC and the Linux Cluster of the Leibniz Supercomputing Center LRZ, Bavarian Academy of Sciences and the Humanities (BAdW), funded via GCS by BMBF and StMWFK.

References

Aalbers, E. E., Lenderink, G., van Meijgaard, E., and van den Hurk, B. J. J. M.: Local-scale changes in mean and heavy precipitation in Western Europe, climate change or internal variability?, Climate Dynamics, 50, 4745–4766, https://doi.org/10.1007/s00382-017-3901-9, 2018.

Abatzoglou, J. T., Juang, C. S., Williams, A. P., Kolden, C. A., and Westerling, A. L.: Increasing Synchronous Fire Danger in Forests of the Western United States, Geophysical Research Letters, 48, https://doi.org/10.1029/2020GL091377, 2021.

Arnell, N. W., Freeman, A., and Gazzard, R.: The effect of climate change on indicators of fire danger in the UK, Environmental Research Letters, 16, 44 027, https://doi.org/https://doi.org/10.1088/1748-9326/abd9f2, 2021.

Bakke, S. J., Wanders, N., van der Wiel, K., and Tallaksen, L. M.: A data-driven model for Fennoscandian wildfire danger, Natural Hazards and Earth System Sciences, 23, 65–89, https://doi.org/10.5194/nhess-23-65-2023, 2023.

Barbero, R., Abatzoglou, J. T., Larkin, N. K., Kolden, C. A., and Stocks, B.: Climate change presents increased potential for very large fires in the contiguous United States, Int. J. Wildland Fire, 24, 892–899, https://doi.org/https://doi.org/10.1071/WF15083, 2015.

Barbero, R., Abatzoglou, J. T., Pimont, F., Ruffault, J., and Curt, T.: Attributing Increases in Fire Weather to Anthropogenic Climate Change Over France, Frontiers in Earth Science, 8, https://doi.org/https://doi.org/10.3389/feart.2020.00104, 2020.

Bowman, D. M. J. S., Kolden, C. A., Abatzoglou, J. T., Johnston, F. H., van der Werf, G. R., and Flannigan, M.: Vegetation fires in the Anthropocene, Nature Reviews Earth and Environment, 1, 500–515, https://doi.org/https://doi.org/10.1038/s43017-020-0085-3, 2020.

~~BR: Landkreis Kronach: Katastrophenfallnach Waldbrandaufgehoben, , 2022.~~

Bradshaw, L. S., Deeming, J. E., Burgan, R. E., and Cohen, J. D.: The 1978 National Fire-Danger Rating System: technical documentation, Tech. rep., https://doi.org/https://doi.org/10.2737/INT-GTR-169, 1984.

Brunner, M. I., Swain, D. L., Wood, R. R., Willkofer, F., Done, J. M., Gilleland, E., and Ludwig, R.: An extremeness threshold determines the regional response of floods to changes in rainfall extremes, Communications Earth & Environment, 2, 1–11, https://doi.org/10.1038/s43247-021-00248-x, 2021.

Brönnimann, S., Rajczak, J., Fischer, E. M., Raible, C. C., Rohrer, M., and Schär, C.: Changing seasonality of moderate and extreme precipitation events in the Alps, Natural Hazards and Earth System Sciences, 18, 2047–2056, https://doi.org/10.5194/nhess-18-2047-2018, 2018.

Böhnisch, A., Ludwig, R., and Leduc, M.: Using a nested single-model large ensemble to assess the internal variability of the North Atlantic Oscillation and its climatic implications for central Europe, Earth System Dynamics, 11, 617–640, https://doi.org/10.5194/esd-11-617-2020, 2020.

Böhnisch, A., Mittermeier, M., Leduc, M., and Ludwig, R.: Hot Spots and Climate Trends of Meteorological Droughts in Europe–Assessing the Percent of Normal Index in a Single-Model Initial-Condition Large Ensemble, Frontiers in Water, 3, 107, https://doi.org/https://doi.org/10.3389/frwa.2021.716621, 2021.

Böhnisch, A., Felsche, E., and Ludwig, R.: European heatwave tracks: using causal discovery to detect recurring pathways in a single-regional climate model large ensemble, Environmental Research Letters, 18, https://doi.org/10.1088/1748-9326/aca9e3, 2023.

Cannon, A. J.: Multivariate quantile mapping bias correction: an N-dimensional probability density function transform for climate model simulations of multiple variables, Climate Dynamics, 50, 31–49, https://doi.org/10.1007/s00382-017-3580-6, 2018.

CLMS: Corine Land Cover 2018, Version 2020-20u1, Tech. rep., Corine Land Management Service (CLMS), https://land.copernicus.eu/pan-european/corine-land-cover/clc2018?tab=metadata, last access 10/13/2021, 2021.

Coles, S.: An Introduction to Statistical Modeling of Extreme Values, Springer Series in Statistics, Springer, London, https://doi.org/10.1007/978-1-4471-3675-0, 2001.

Conedera, M., Krebs, P., Valese, E., Cocca, G., Schunk, C., Menzel, A., Vacik, H., Cane, D., Japelj, A., Muri, B., Ricotta, C., Oliveri, S., and Pezzatti, G. B.: Characterizing Alpine pyrogeography from fire statistics, Applied Geography, 98, 87–99, https://doi.org/10.1016/j.apgeog.2018.07.011, 2018.

De Rigo, D., Libertà, G., Houston Durrant, T., Artés Vivancos, T., and San-Miguel-Ayanz, J.: Forest fire danger extremes in Europe under climate change: variability and uncertainty., Tech. rep., Publications Office of the European Union, https://doi.org/https://doi.org/10.2760/13180, 2017.

Deser, C., Knutti, R., Solomon, S., and Phillips, A. S.: Communication of the role of natural variability in future North American climate, Nature Climate Change, 2, 775–779, https://doi.org/10.1038/nclimate1562, 2012.

Deser, C., Lehner, F., Rodgers, K. B., Ault, T., Delworth, T. L., DiNezio, P. N., Fiore, A., Frankignoul, C., Fyfe, J. C., Horton, D. E., Kay, J. E., Knutti, R., Lovenduski, N. S., Marotzke, J., McKinnon, K. A., Minobe, S., Randerson, J., Screen, J. A., Simpson, I. R., and Ting, M.: Insights from Earth system model initial-condition large ensembles and future prospects, Nature Climate Change, 10, 277–286, https://doi.org/10.1038/s41558-020-0731-2, 2020.

Di Giuseppe, F., Pappenberger, F., Wetterhall, F., Krzeminski, B., Camia, A., Libertá, G., and San Miguel, J.: The Potential Predictability of Fire Danger Provided by Numerical Weather Prediction, Journal of Applied Meteorology and Climatology, 55, 2469–2491, https://doi.org/https://doi.org/10.1175/JAMC-D-15-0297.1, 2016.

EFFIS: Fire Danger Forecast, Tech. rep., European Forest Fire Information System, https://effis.jrc.ec.europa.eu/about-effis/technical-background/fire-danger-forecast, last access 12/21/2021, 2021.

Fargeon, H., Pimont, F., Martin-StPaul, N., De Caceres, M., Ruffault, J., Barbero, R., and Dupuy, J.-L.: Projections of fire danger under climate change over France: where do the greatest uncertainties lie?, Climatic Change, 160, 479–493, https://doi.org/https://doi.org/10.1007/s10584-019-02629-w, 2020.

Felsche, E., Böhnisch, A., and Ludwig, R.: Inter-seasonal connection of typical European heatwave patterns to soil moisture, npj Climate and Atmospheric Science, 6, 1–11, https://doi.org/10.1038/s41612-023-00330-5, 2023.

Fischer, E. M., Beyerle, U., and Knutti, R.: Robust spatially aggregated projections of climate extremes, Nature Climate Change, 3, 1033–1038, https://doi.org/10.1038/nclimate2051, 2013.

Fyfe, J. C., Derksen, C., Mudryk, L., Flato, G. M., Santer, B. D., Swart, N. C., Molotch, N. P., Zhang, X., Wan, H., Arora, V. K., Scinocca, J., and Jiao, Y.: Large near-term projected snowpack loss over the western United States, Nature Communications, 8, ~~14 996,~~ https://doi.org/https://doi.org/10.1038/ncomms14996, 2017.

Giannaros, T. M., Papavasileiou, G., Lagouvardos, K., Kotroni, V., Dafis, S., Karagiannidis, A., and Dragozi, E.: Meteorological Analysis of the 2021 Extreme Wildfires in Greece: Lessons Learned and Implications for Early Warning of the Potential for Pyroconvection, Atmosphere, 13, https://doi.org/10.3390/atmos13030475, 2022.

Gillett, N. P., Cannon, A. J., Malinina, E., Schnorbus, M., Anslow, F., Sun, Q., Kirchmeier-Young, M., Zwiers, F., Seiler, C., Zhang, X., Flato, G., Wan, H., Li, G., and Castellan, A.: Human influence on the 2021 British Columbia floods, Weather and Climate Extremes, 36, ~~100 441,~~ https://doi.org/https://doi.org/10.1016/j.wace.2022.100441, 2022.

Hawkins, E.: Warming Stripes, Tech. rep., https://www.climate-lab-book.ac.uk/2018/warming-stripes/, 2018.

Hawkins, E. and Sutton, R.: The Potential to Narrow Uncertainty in Regional Climate Predictions, Bulletin of the American Meteorological Society, 90, 1095 – 1108, https://doi.org/https://doi.org/10.1175/2009BAMS2607.1, 2009.

Hoffman, K. M., Christianson, A. C., Gray, R. W., and Daniels, L.: Western Canada's new wildfire reality needs a new approach to fire management, Environmental Research Letters, 17, 061 001, https://doi.org/10.1088/1748-9326/ac7345, 2022.

IPCC: Summary for Policymakers. In: Climate Change 2021: The Physical Science Basis. Contribution of Working Group I to the Sixth Assessment Report of the Intergovernmental Panel on Climate Change, Cambridge University Press, Cambridge, United Kingdom and New York, USA, 2021.

Kay, J. E., Deser, C., Phillips, A., Mai, A., Hannay, C., Strand, G., Arblaster, J. M., Bates, S. C., Danabasoglu, G., Edwards, J., Holland, M., Kushner, P., Lamarque, J.-F., Lawrence, D., Lindsay, K., Middleton, A., Munoz, E., Neale, R., Oleson, K., Polvani, L., and Vertenstein, M.: The Community Earth System Model (CESM) Large Ensemble Project: A Community Resource for Studying Climate Change in the Presence of Internal Climate Variability, Bulletin of the American Meteorological Society, 96, 1333–1349, , 2015.

Kirchmeier-Young, M. C., Zwiers, F. W., Gillett, N. P., and Cannon, A. J.: Attributing extreme fire risk in Western Canada to human emissions, Climatic Change, 144, 365–379, https://doi.org/https://doi.org/10.1007/s10584-017-2030-0, 2017.

Landesamt für Umwelt: Naturräumliche Gliederung Bayerns - LfU Bayern, https://www.lfu.bayern.de/natur/naturraeume/index.htm, 2023.

Leduc, M., Mailhot, A., Frigon, A., Martel, J.-L., Ludwig, R., Brietzke, G. B., Giguère, M., Brissette, F., Turcotte, R., Braun, M., and Scinocca, J.: The ClimEx Project: A 50-Member Ensemble of Climate Change Projections at 12-km Resolution over Europe and North-eastern North America with the Canadian Regional Climate Model (CRCM5), Journal of Applied Meteorology and Climatology, 58, 663–693, https://doi.org/10.1175/JAMC-D-18-0021.1, 2019.

Maher, N., Milinski, S., and Ludwig, R.: Large ensemble climate model simulations: introduction, overview, and future prospects for utilising multiple types of large ensemble, Earth System Dynamics, 12, 401–418, , 2021.

Martynov, A., Laprise, R., Sushama, L., Winger, K., Šeparović, L., and Dugas, B.: Reanalysis-driven climate simulation over CORDEX North America domain using the Canadian Regional Climate Model, version 5: model performance evaluation, Climate Dynamics, 41, 2973–3005, https://doi.org/10.1007/s00382-013-1778-9, 2013.

McArthur, A. G.: Weather and grassland fire behaviour, Forestry and Timber Bureau, 1966.

Mittermeier, M., Braun, M., Hofstätter, M., Wang, Y., and Ludwig, R.: Detecting Climate Change Effects on Vb Cyclones in a 50-Member Single-Model Ensemble Using Machine Learning, Geophysical Research Letters, 46, 14 653–14 661, https://doi.org/https://doi.org/10.1029/2019GL084969, 2019.

Mpelasoka, F. S. and Chiew, F. H. S.: Influence of Rainfall Scenario Construction Methods on Runoff Projections, Journal of Hydrometeorology, 10, 1168 – 1183, https://doi.org/https://doi.org/10.1175/2009JHM1045.1, 2009.

Pausas, J. G. and Paula, S.: Fuel shapes the fire–climate relationship: evidence from Mediterranean ecosystems, Global Ecology and Biogeography, 21, 1074–1082, https://doi.org/10.1111/j.1466-8238.2012.00769.x, 2012.

Piani, C., Haerter, J. O., and Coppola, E.: Statistical bias correction for daily precipitation in regional climate models over Europe, Theoretical and Applied Climatology, 99, 187–192, https://doi.org/10.1007/s00704-009-0134-9, 2010.

Poschlod, B., Willkofer, F., and Ludwig, R.: Impact of Climate Change on the Hydrological Regimes in Bavaria, Water, 12, https://doi.org/https://doi.org/10.3390/w12061599, 2020.

Ruffault, J., Moron, V., Trigo, R. M., and Curt, T.: Daily synoptic conditions associated with large fire occurrence in Mediterranean France: evidence for a wind-driven fire regime, International Journal of Climatology, 37, 524–533, https://doi.org/https://doi.org/10.1002/joc.4680, 2017.

Ruffault, J., Curt, T., Moron, V., Trigo, R. M., Mouillot, F., Koutsias, N., Pimont, F., Martin-StPaul, N., Barbero, R., Dupuy, J.-L., Russo, A., and Belhadj-Khedher, C.: Increased likelihood of head-induced large wildfires in the Mediterrranean, Scientific Reports, 10, 13 790, https://doi.org/https://doi.org/10.1038/s41598-020-70069-z, 2020.

San-Miguel-Ayanz, J., Costa, H., de Rigo, D., Libertà, G., Vivancos, T. A., Tracy Durrant, D. N., Löffler, P., and Moore, P.: Basic criteria to assess wildfire risk at the Pan-European level, Tech. rep., https://ec.europa.eu/jrc/en/publication/basic-criteria-assess-wildfire-risk-pan-european-level, last acess 12/12/2021, 2018.

~~Spiegel: Waldbrand in~~

Separović, L., Alexandru, A., Laprise, R., Martynov, A., Sushama, L., Winger, K., Tete, K., and Valin, M.: Present climate and climate change over ~~Treuenbrietzen~~North ~~: Hunderte~~America ~~müssen ihre~~ as simulated by the fifth-generation ~~Häuser~~Canadian ~~verlassen, Der Spiegel, , 2022.~~

~~StMLF, Landwirtschaft und Forsten, B.S.f. E.: Richtlinie zur Waldbrandabwehr~~regional climate model, Climate Dynamics, 41, ~~,~~ 3167–3201, https://doi.org/10.1007/s00382-013-1737-5, 2013.

Touma, D., Stevenson, S., Lehner, F., and Coats, S.: Human-driven greenhouse gas and aerosol emissions cause distinct regional impacts on extreme fire weather, Nature Communications, 12, 212, https://doi.org/https://doi.org/10.1038/s41467-020-20570-w, 2021.

Turco, M., Rosa-Cánovas, J. J., Bedia, J., Jerez, S., Montávez, J. P., Llasat, M. C., and Provenzale, A.: Exacerbated fires in Mediterranean Europe due to anthropogenic warming projected with non-stationary climate-fire models, Nature Communications, 9, 3821, https://doi.org/https://doi.org/10.1038/s41467-018-06358-z, 2018.

~~Van~~

van Wagner, C. E.: Development and structure of the Canadian Forest Fire Weather Index System, Tech. rep., https://cfs.nrcan.gc.ca/publications?id=19927, 1987.

~~Van~~

van Wagner, C. E. and Pickett, T. L.: Equations and FORTRAN Program for the Canadian Forest Fire Weather Index System, Tech. rep., Canadian Forestry Service, Ottawa, 1985.

Virtanen, P., Gommers, R., Oliphant, T. E., Haberland, M., Reddy, T., Cournapeau, D., Burovski, E., Peterson, P., Weckesser, W., Bright, J., van der Walt, S. J., Brett, M., Wilson, J., Millman, K. J., Mayorov, N., Nelson, A. R. J., Jones, E., Kern, R., Larson, E., Carey, C. J., Polat, İ., Feng, Y., Moore, E. W., VanderPlas, J., Laxalde, D., Perktold, J., Cimrman, R., Henriksen, I., Quintero, E. A., Harris, C. R., Archibald, A. M., Ribeiro, A. H., Pedregosa, F., van Mulbregt, P., and SciPy 1.0 Contributors: SciPy 1.0: Fundamental Algorithms for Scientific Computing in Python, Nature Methods, 17, 261–272, https://doi.org/10.1038/s41592-019-0686-2, 2020.

Vitolo, C., Di Giuseppe, F., Krzeminski, B., and San-Miguel-Ayanz, J.: A 1980-2018 global fire danger re-analysis dataset for the Canadian Fire Weather Indices, Scientific Data, 6, 190 032, https://doi.org/https://doi.org/10.1038/sdata.2019.32, 2019.

Vitolo, C., Di Giuseppe, F., Barnard, C., Coughlan, R., San-Miguel-Ayanz, J., Libertá, G., and Krzeminski, B.: ERA5-based global meteorological wildfire danger maps, Scientific Data, 7, 216, https://doi.org/10.1038/s41597-020-0554-z, 2020.

~~Von~~

von Trentini, F., Leduc, M., and Ludwig, R.: Assessing natural variability in RCM signals: comparison of a multi model EURO-CORDEX ensemble with a 50-member single model large ensemble, Climate Dynamics, 53, 1963–1979, https://doi.org/https://doi.org/10.1007/s00382-019-04755-8, 2019.

von Trentini, F., Aalbers, E. E., Fischer, E. M., and Ludwig, R.: Comparing interannual variability in three regional single-model initial-condition large ensembles (SMILEs) over Europe, Earth System Dynamics, 11, 1013–1031, https://doi.org/10.5194/esd-11-1013-2020, 2020.

Vrac, M.: Multivariate bias adjustment of high-dimensional climate simulations: the Rank Resampling for Distributions and Dependences (R^2D^2) bias correction, Hydrology and Earth System Sciences, 22, 3175–3196, https://doi.org/10.5194/hess-22-3175-2018, 2018.

Wang, X., Wotton, B. M., Cantin, A. S., Parisien, M.-A., Anderson, K., Moore, B., and Flannigan, M. D.: cffdrs: an R package for the Canadian Forest Fire Danger Rating System, Ecological Processes, 6, 5, https://doi.org/https://doi.org/10.1186/s13717-017-0070-z, 2017.

Wastl, C., Schunk, C., Leuchner, M., Pezzatti, G. B., and Menzel, A.: Recent climate change: Long-term trends in meteorological forest fire danger in the Alps, Agricultural and Forest Meteorology, 162-163, 1–13, https://doi.org/10.1016/j.agrformet.2012.04.001, 2012.

Willkofer, F., Wood, R. R., von Trentini, F., Weismüller, J., Poschlod, B., and Ludwig, R.: A Holistic Modelling Approach for the Estimation of Return Levels of Peak Flows in Bavaria, Water, 12, https://doi.org/https://doi.org/10.3390/w12092349, 2020.

Wood, R. R.: Role of mean and variability change in changes in European annual and seasonal extreme precipitation events, Earth System Dynamics, 14, 797–816, https://doi.org/10.5194/esd-14-797-2023, 2023.

Wood, R. R. and Ludwig, R.: Analyzing Internal Variability and Forced Response of Subdaily and Daily Extreme Precipitation Over Europe, Geophysical Research Letters, 47, https://doi.org/10.1029/2020GL089300, 2020.

Wotton, B. M.: Interpreting and using outputs from the Canadian Forest Fire Danger Rating System in research applications, Environmental and Ecological Statistics, 16, 107–131, https://doi.org/https://doi.org/10.1007/s10651-007-0084-2, 2009.

Yang, W., Gardelin, M., Olsson, J., and Bosshard, T.: Multi-variable bias correction: application of forest fire risk in present and future climate in Sweden, Natural Hazards and Earth System Sciences, 15, 2037–2057, https://doi.org/10.5194/nhess-15-2037-2015, publisher:Copernicus GmbH, 2015.

Šeparović, L., Alexandru, A., Laprise, R., Martynov, A., Sushama, L., Winger, K., Tete, K., and Valin, M.: Present climate and climate change over NorthAmericaas simulated by the fifth-generation Canadianregional climate model, Climate Dynamics, 41, 3167–3201, , 2013.

Zscheischler, J., Fischer, E. M., and Lange, S.: The effect of univariate bias adjustment on multivariate hazard estimates, Earth System Dynamics, 10, 31–43, https://doi.org/10.5194/esd-10-31-2019, 2019.

Appendix A

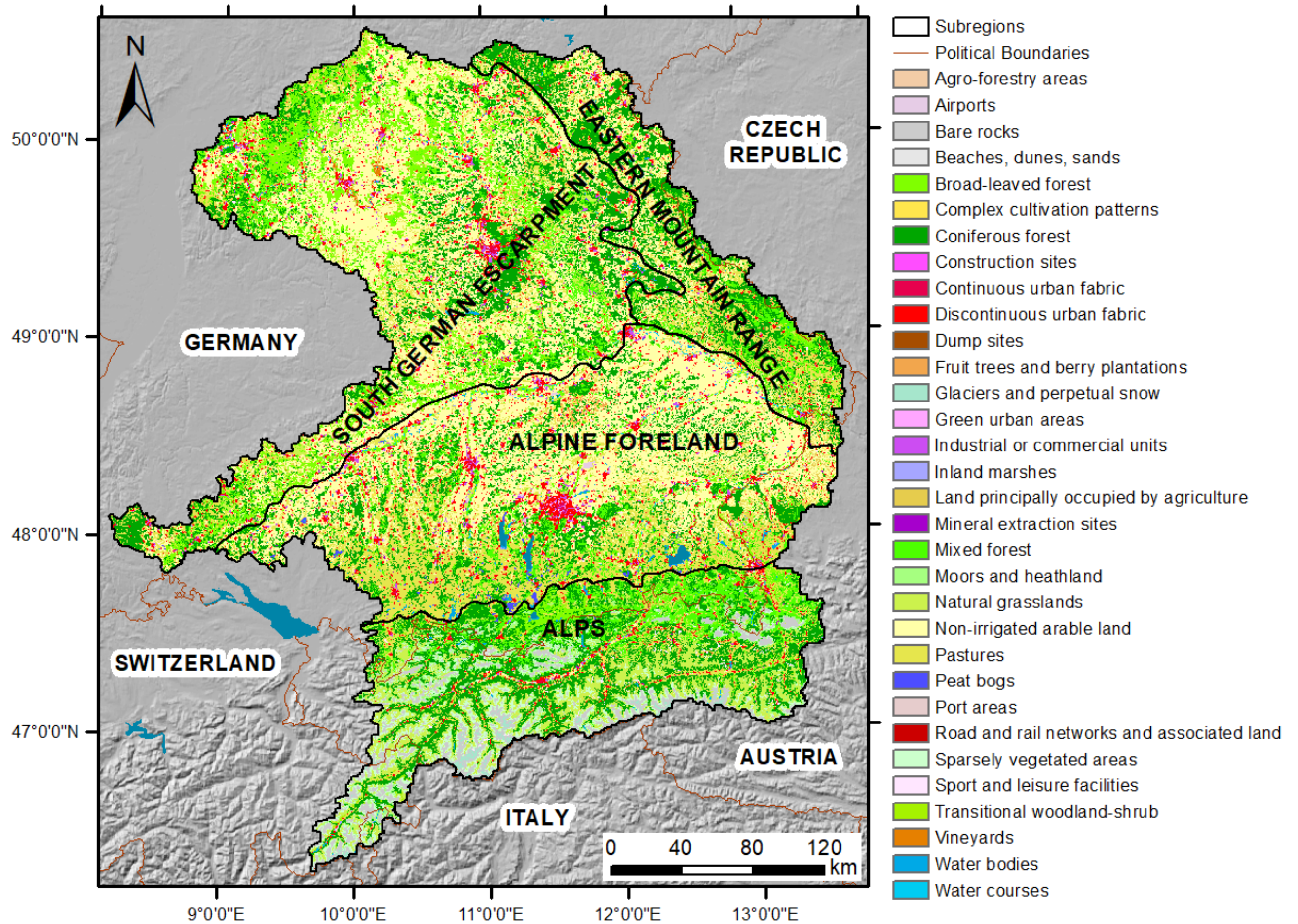

Figure A1. Land cover distribution in Hydrological Bavaria (modified, CLMS (2021))

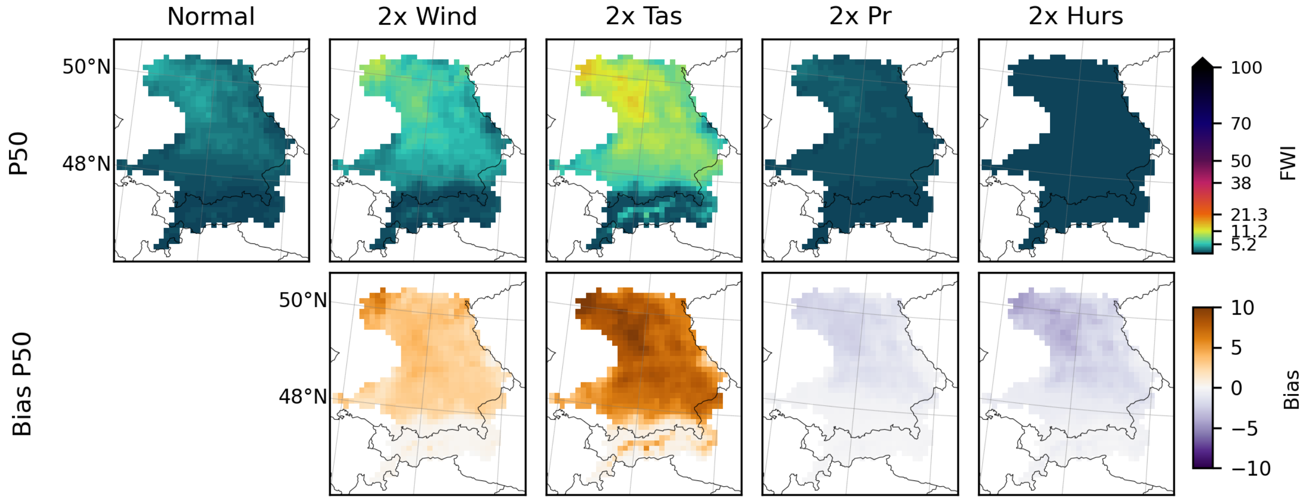

Figure A2. FWI median (top, 50~~th percentile~~th quantile) and bias (bottom) of sensitivity runs, where each input variable is increased by a factor of two (e. g. 2x wind) and the original FWI run (Normal) in the validation period 1981 to 2010. Bias is calculated by subtracting each increased sensitivity run from the original FWI run.

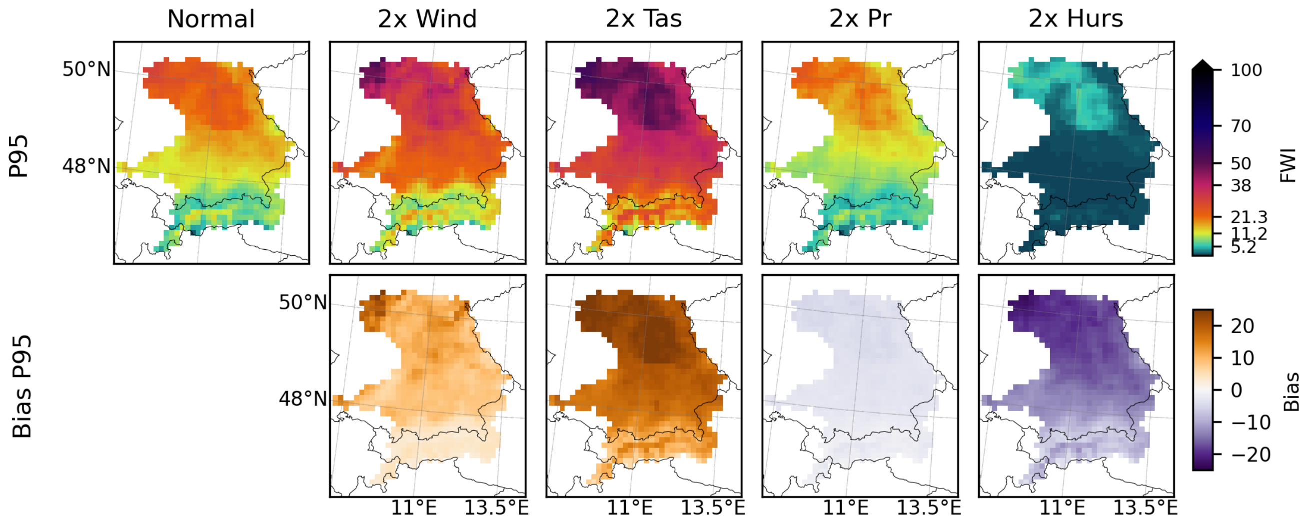

Figure A3. FWI extreme (top, 95~~th percentile~~th quantile) and bias (bottom) of sensitivity runs, where each input variable is increased by a factor of two (e. g. 2x wind) and the original FWI run (Normal) in the validation period 1981 to 2010. Bias is calculated by subtracting each increased sensitivity run from the original FWI run.

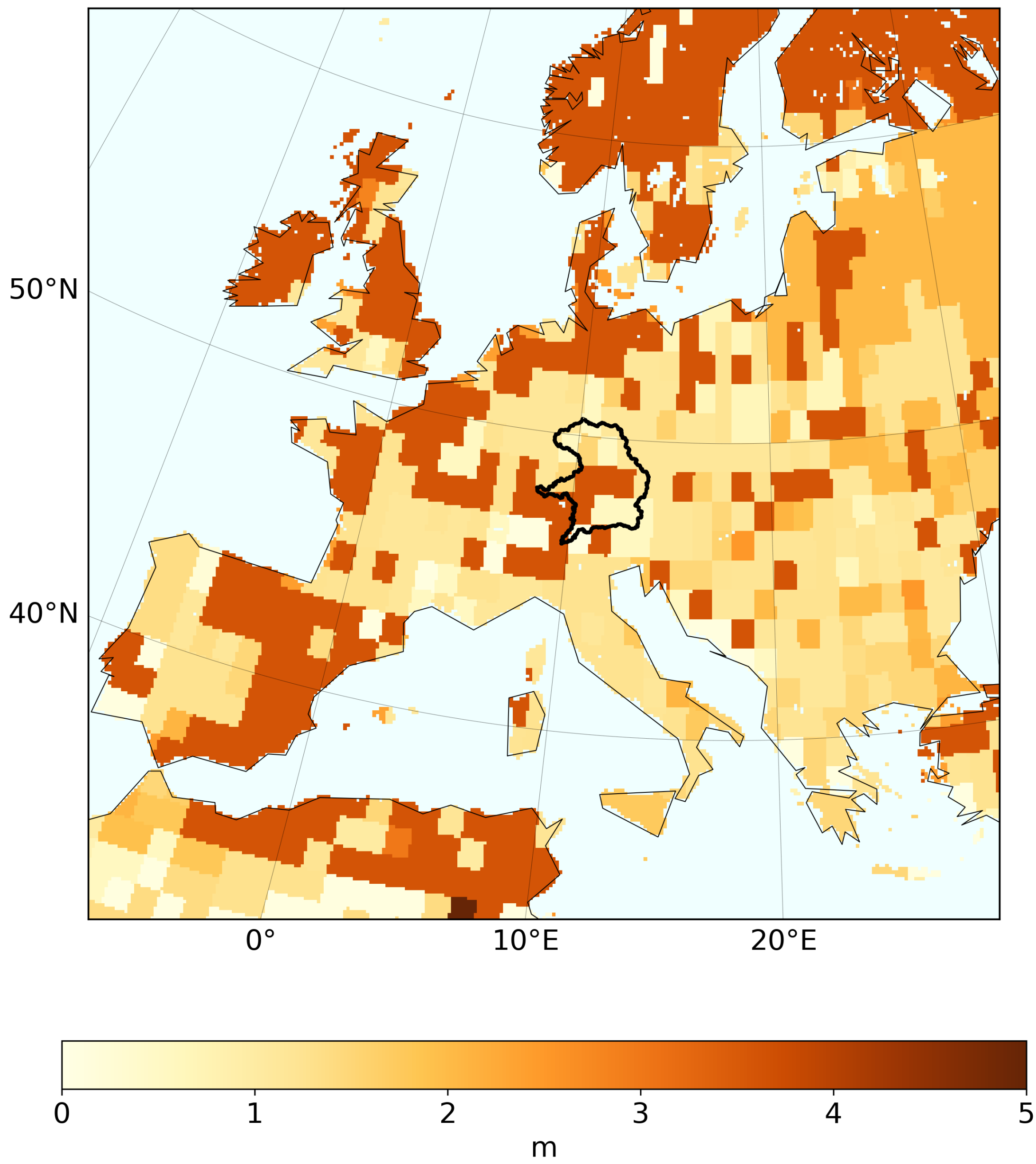

Figure A4. Bedrock depth in the CanESM2 and boundaries of Hydrological Bavaria (black).